



Interactions of Particles with Matter

Nikolai Mokhov, Fermilab

The CERN Accelerator School

21 February – 6 March 2018, Zurich, Switzerland

Outline

- Introduction
- Landscape
- Materials Under Irradiation
- Particle Production in Nuclear Reactions
- Electromagnetic Interactions
- Muon Specifics
- Beam-Induced Effects in Organic and Non-Organic Materials and in Electronics
- Coherent Beam Interactions with Crystals
- Moving Forward

Acknowledgements: F. Cerutti, A. Ferrari, A. Fedynitch, K. Gudima, S. Striganov

Introduction

The consequences of controlled and uncontrolled impacts of high-intensity or/and high-power or/and high-energy beams on components of accelerators, beamlines, target stations, beam collimators, absorbers, detectors, shielding, and environment can range from minor to catastrophic.

Strong, weak, electromagnetic and even gravitational forces (neutron oscillation and neutron TOF experiments) govern high-energy beam interactions with complex components in presence of electromagnetic fields → simulations are only possible with a few well-established Monte-Carlo codes (no analytic or simplified approaches are used these days).

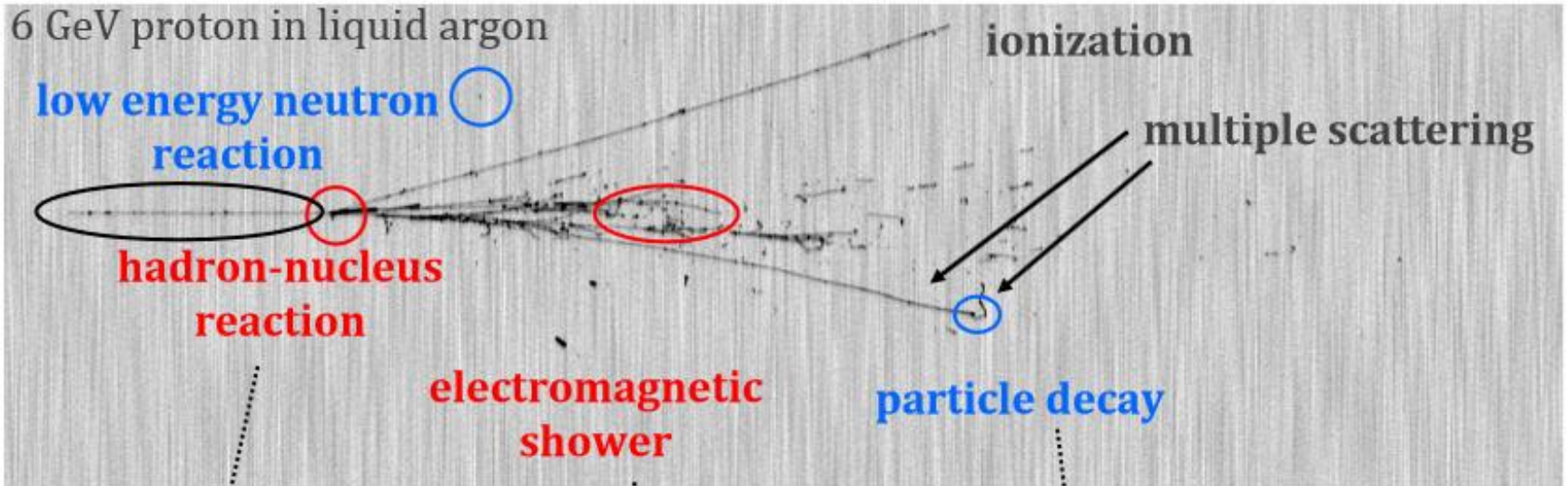
Predictive power and reliability of particle transport simulation tools and physics models in the multi-TeV region should be well-understood and justified to allow for viable designs of future colliders with a minimal risk and a reasonable safety margin.

Interactions of Fast Particles with Matter

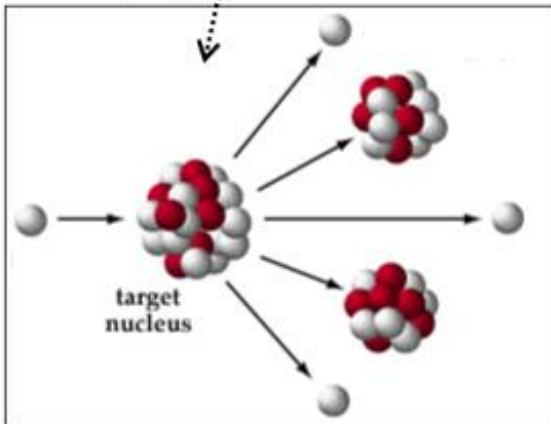
Electromagnetic interactions, decays of unstable particles and strong inelastic and elastic nuclear interactions all affect the passage of high-energy particles through matter. At high energies the characteristic feature of the phenomenon is creation of hadronic cascades and electromagnetic showers (EMS) in matter due to multi-particle production in electromagnetic and strong nuclear interactions.

Because of consecutive multiplication, the interaction avalanche rapidly accrues, passes the maximum and then dies as a result of energy dissipation between the cascade particles and due to ionization energy loss. Energetic particles are concentrated around the projectile axis forming the shower core. Neutral particles (mainly neutrons) and photons dominate with a cascade development when energy drops below a few hundred MeV.

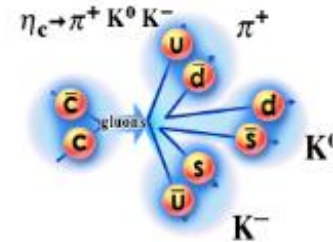
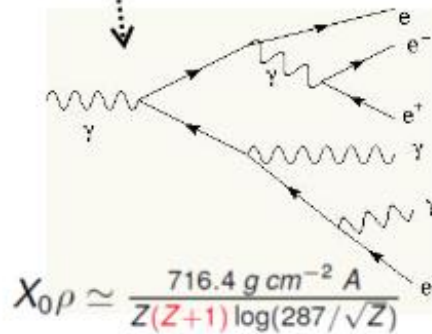
Microscopic View



$$\lambda\rho = \frac{A}{\sigma_R N_A} \quad \sigma_R \simeq \pi r_0^2 A^{2/3}$$



interplay of many physical processes described by different theories/models



Scales of Cascades and Particle Propagation

The length scale in hadronic cascades is a nuclear interaction length λ_I (16.8 cm in iron) while in EMS it is a radiation length X_0 (1.76 cm in iron). The hadronic cascade longitudinal dimension is (5-10) λ_I , while in EMS it is (10-30) X_0 . It grows logarithmically with primary energy in both cases. Transversely, the effective radius of hadronic cascade is about λ_I , while for EMS it is about $2r_M$, where r_M is a Moliere radius $R_M = 0.0265 X_0 (Z+1.2)$. Low-energy neutrons coupled to photons propagate much larger distance in matter around cascade core, both longitudinally and transversely, until they dissipate their energy in a region of a fraction of an electronvolt.

Muons - created predominantly in pion and kaon decays during the cascade development – can travel hundreds and thousands of meters in matter along the cascade axis. Neutrinos – usual muon partners in such decays – propagate even farther, hundreds and thousands of kilometers, until they exit the Earth's surface.

Materials Under Irradiation

Depending on material, level of energy deposition density and its time structure, one can face a variety of effects in materials under impact of directly particle beams or radiation induced by them.

Component damage (lifetime):

- Thermal shocks and quasi-instantaneous damage
- Insulation property deterioration due to dose buildup
- Radiation damage to inorganic materials due to atomic displacements and helium production

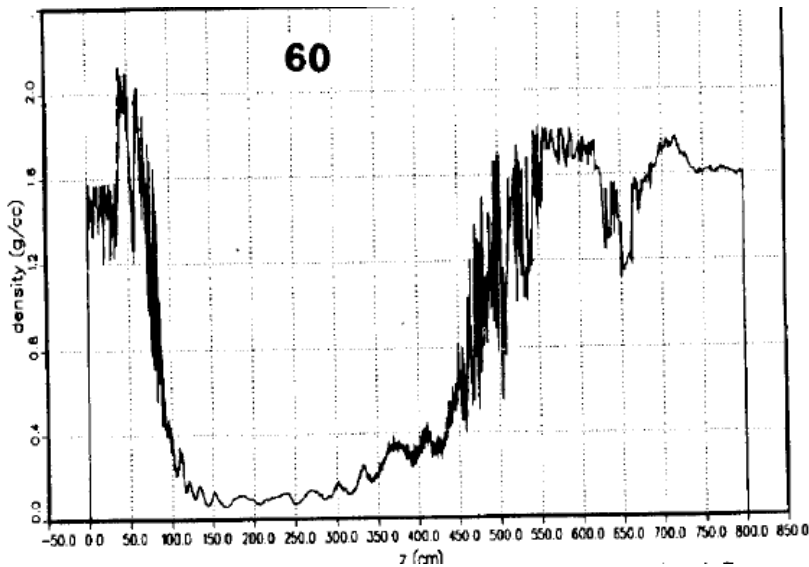
Operational (performance):

- Superconducting magnet quench
- Single-event upset and other soft errors in electronics
- Detector performance deterioration
- Radioactivation, prompt dose and impact on environment

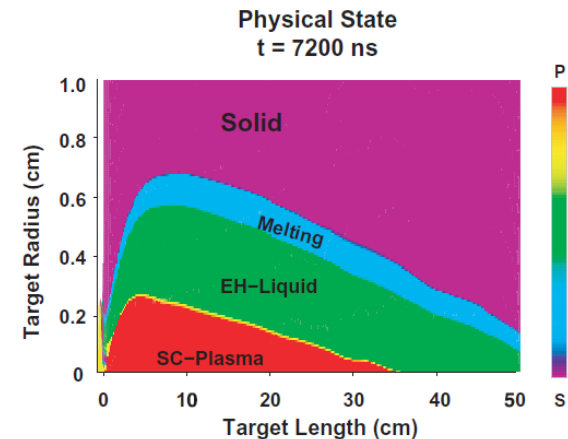
Hydrodynamics in Solid Materials

Pulses with EDD >15 kJ/g: hydrodynamic regime.

First done for the 300- μ s, 400-MJ, 20-TeV proton beams for the SSC graphite beam dump, steel collimators and tunnel-surrounding Austin Chalk by SSC-LANL Collaboration (D. Wilson, ..., N. Mokhov, PAC93, p. 3090). Combining MARS ED calculations at each time step for a fresh material state and MESA/SPHINX hydrodynamics codes.



The hole was drilled at the 7 cm/ μ s penetration rate. Shown is axial density of graphite beam dump in 60 μ s after the spill start



Later, studies by N. Tahir et al with FLUKA+BIG2 codes for SPS & LHC

These days we use MARS+FRONTIER

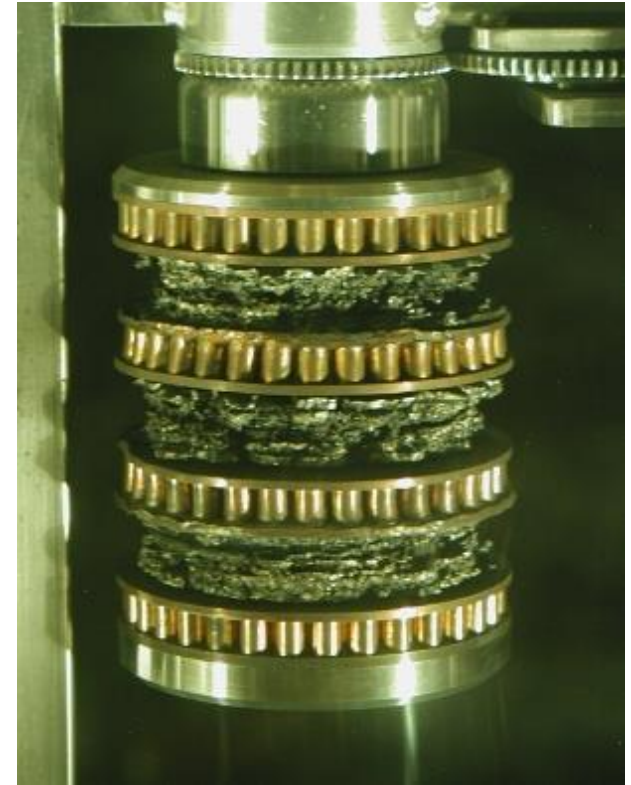
Thermal Shock

Short pulses with energy deposition density EDD in the range from 200 J/g (W), 600 J/g (Cu), ~1 kJ/g (Ni, Inconel) to ~15 kJ/g: thermal shocks resulting in fast ablation and slower structural changes.



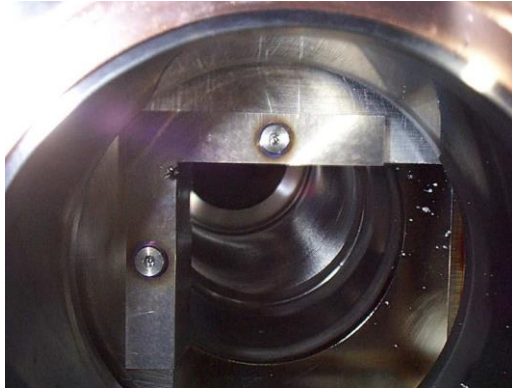
FNAL pbar production target under 120-GeV p-beam ($3e12$ ppp, $\sigma \sim 0.2$ mm)

MARS simulations explained target damage, reduction of pbar yield and justified better target materials

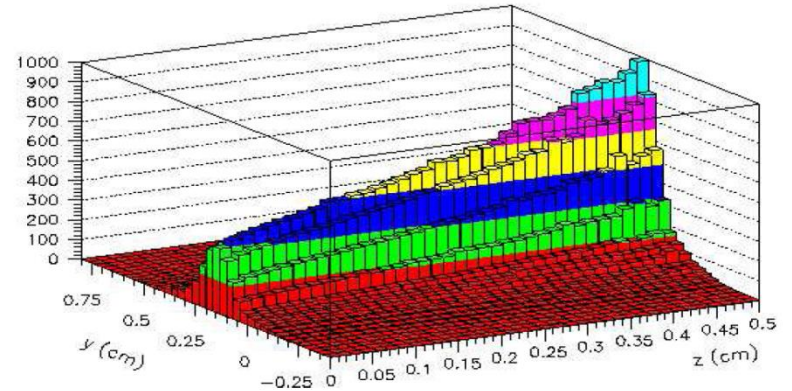
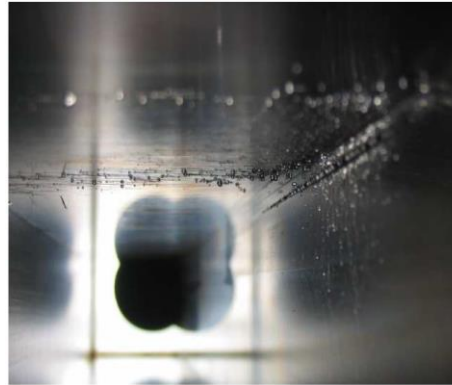


Tevatron Tungsten Collimator Ablation

Hole in 5-mm W



25-cm groove in SS



Detailed modeling of dynamics of beam loss (STRUCT), energy deposition (MARS15) as high as 1 kJ/g, and time evolution over 1.6 ms of the tungsten collimator ablation, fully explained what happened

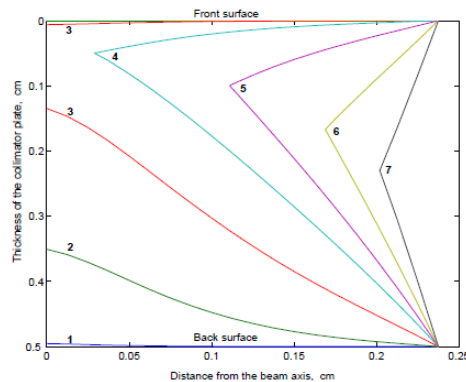
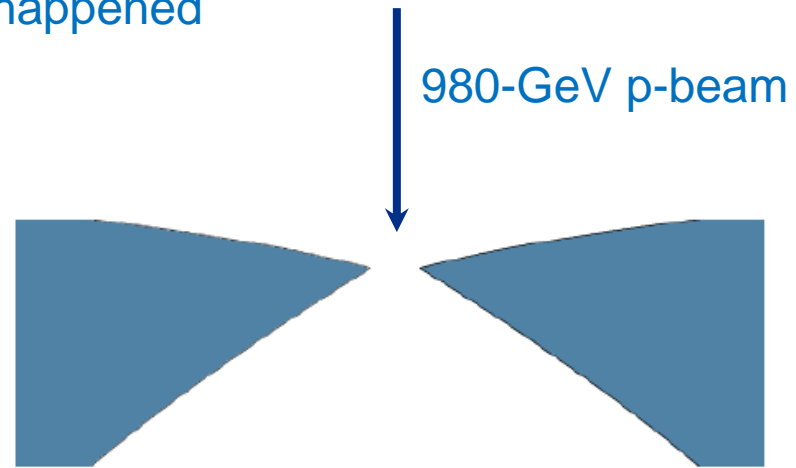


Figure 7: Evolution of the front and back surfaces of the collimator plate at $t = 0.4_{[1]} - 1.6_{[7]} \text{ ms}$ with $\Delta t = 0.2 \text{ ms}$.

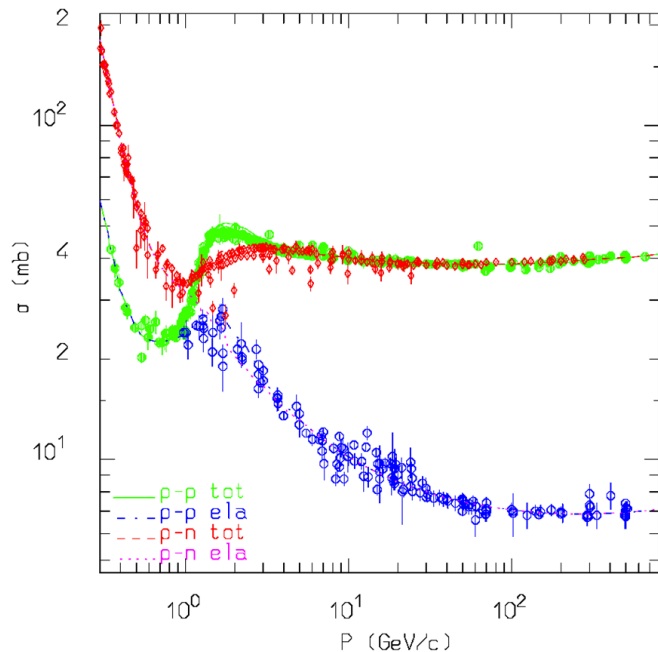


There are Two Kinds of Nuclear Reactions

- **Elastic interactions** are those that **do not change the internal structure** of the projectile/target and **do not produce new particles**. Their effect is to transfer part of the projectile energy to the target (lab system), or equivalently to deflect in opposite directions target and projectile in the Centre-of-Mass system with no change in their energy. There is no threshold for elastic interactions.
- **Non-elastic reactions** are those where **new particles are produced** and/or the **internal structure** of the projectile/target **is changed** (e.g. exciting a nucleus). **These reactions are the origin of the majority of beam-induced deleterious effects** in accelerator, detector, beamlines, targets, collimators, absorbers and environment. A specific non-elastic reaction has usually an energy threshold below which it cannot occur (the exception being neutron capture).

Non-Elastic Hadron-Nucleon Reactions

In order to understand Hadron-Nucleus (hA) nuclear reactions, one has to understand first Hadron-Nucleon (hN) reactions, since nuclei are made up by protons and neutrons.



Intermediate Energies

All reactions proceed through an intermediate state containing at least one resonance (dominance of the $\Delta(1232)$ resonance and of the N^* resonances)

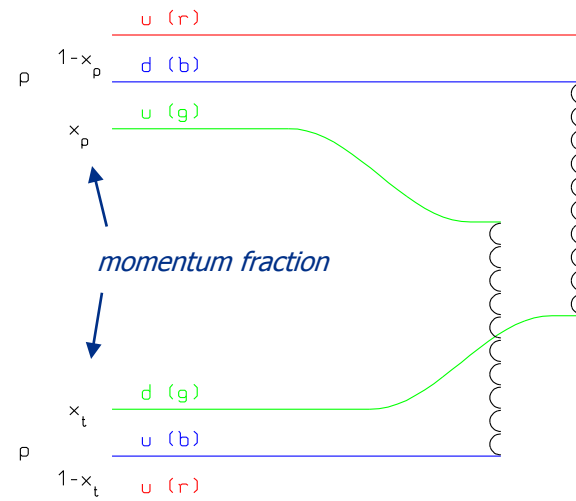
$N_1 + N_2 \rightarrow N_1' + N_2' + \pi$ threshold around 290 MeV,
important above 700 MeV

$\pi + N \rightarrow \pi' + \pi'' + N'$ opens at 170 MeV

High Energies: Dual Parton Model/Quark Gluon String Model etc

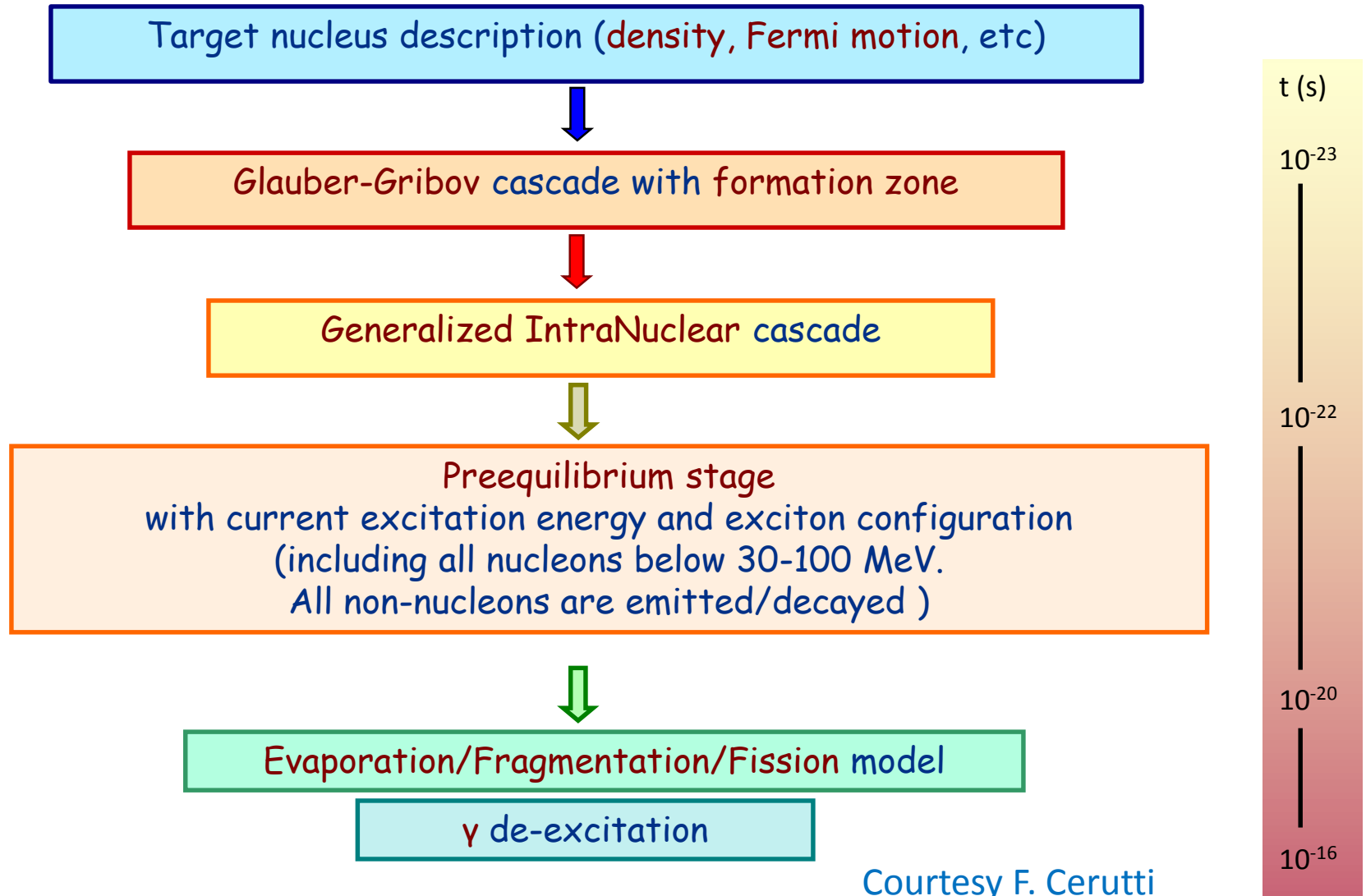
Interacting strings (quarks held together by the gluon-gluon interaction into the form of a string). Each of the two hadrons splits into 2 colored partons \rightarrow combination into 2 colorless chains \rightarrow 2 back-to-back jets.

Each jet is then hadronized into physical hadrons.



Courtesy F. Cerutti

Non-Elastic Hadron-Nucleus Reactions



Status of Particle Production Theoretical Models

- Except for the very first multi-TeV beam interactions with matter at LHC and future hadron colliders, the majority of non-elastic nuclear interactions in hadronic cascades takes place still in the GeV and sub-GeV regions.
- Particle production models are OK at $E_p < 1$ GeV, $E_p > 10$ GeV and – with recent improvements - up to LHC energies.
- At intermediate energies 1 - 10 GeV, there are some theoretical difficulties and uncertainties in experimental data; the latter contradicts each other in some cases.

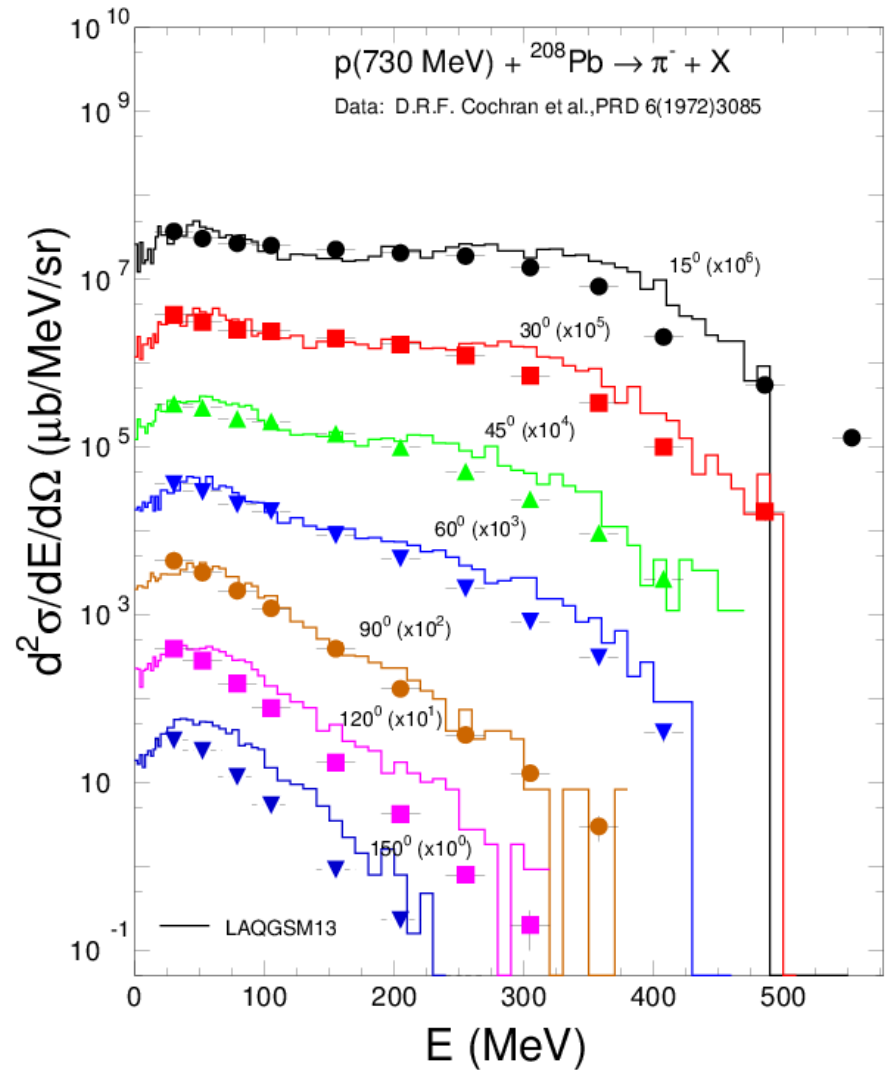
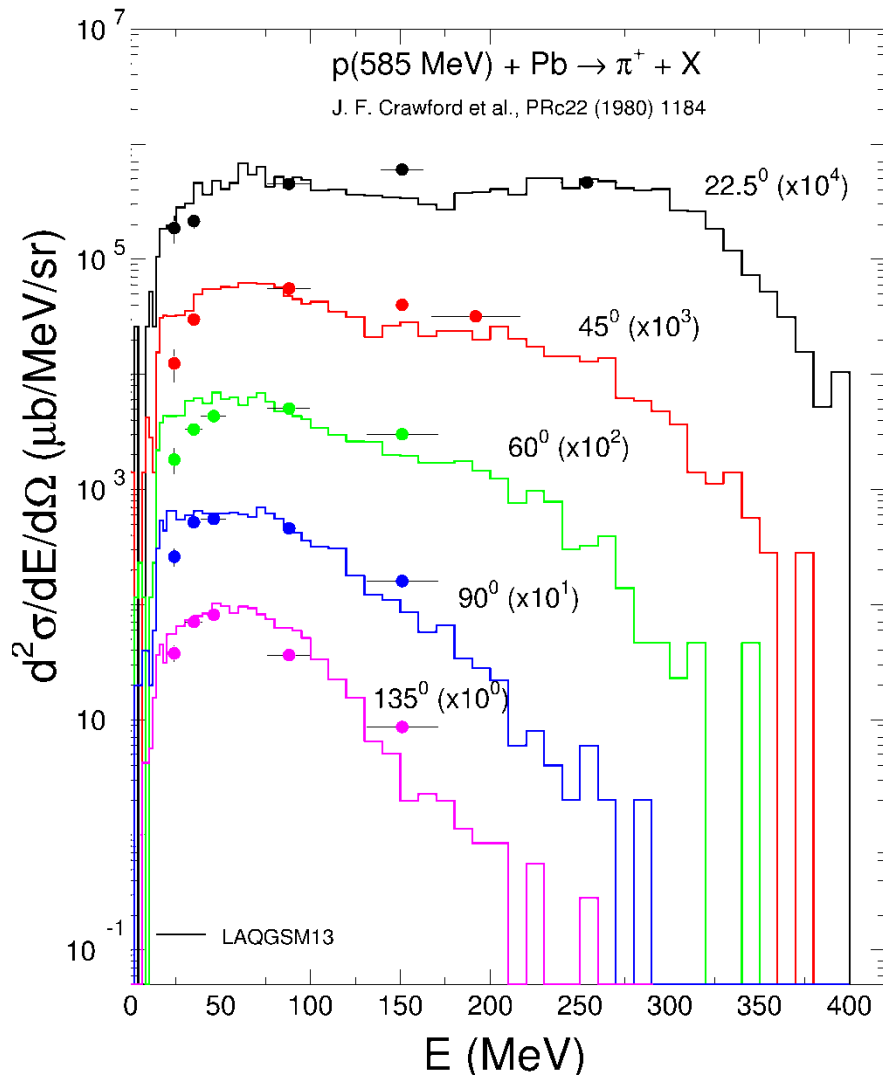
Example: MARS15 Exclusive Event Generator

The Los Alamos Quark-Gluon String Model code, LAQGSM, is used in MARS15 for photon, particle and heavy-ion projectiles at a few MeV/A to 10 TeV/A. This provides a power of full theoretically consistent modeling of exclusive and inclusive distributions of secondary particles, spallation, fission, and fragmentation products.

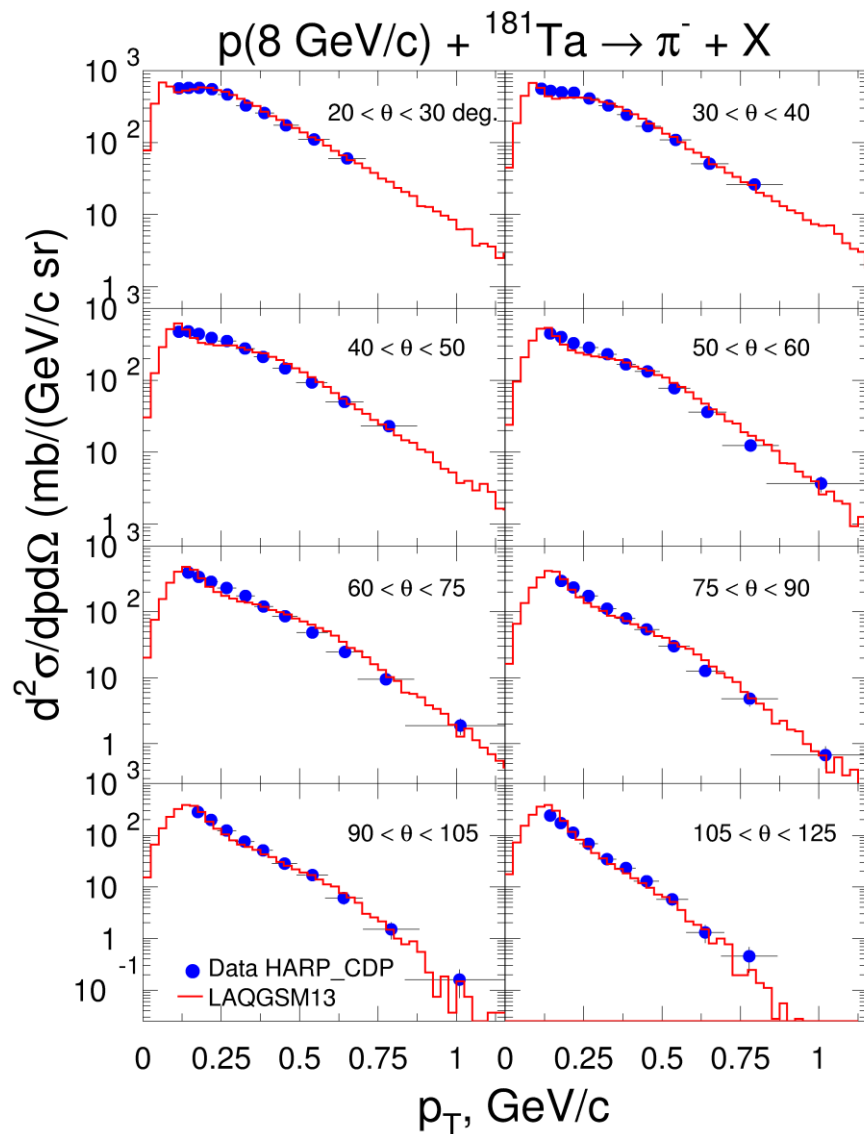
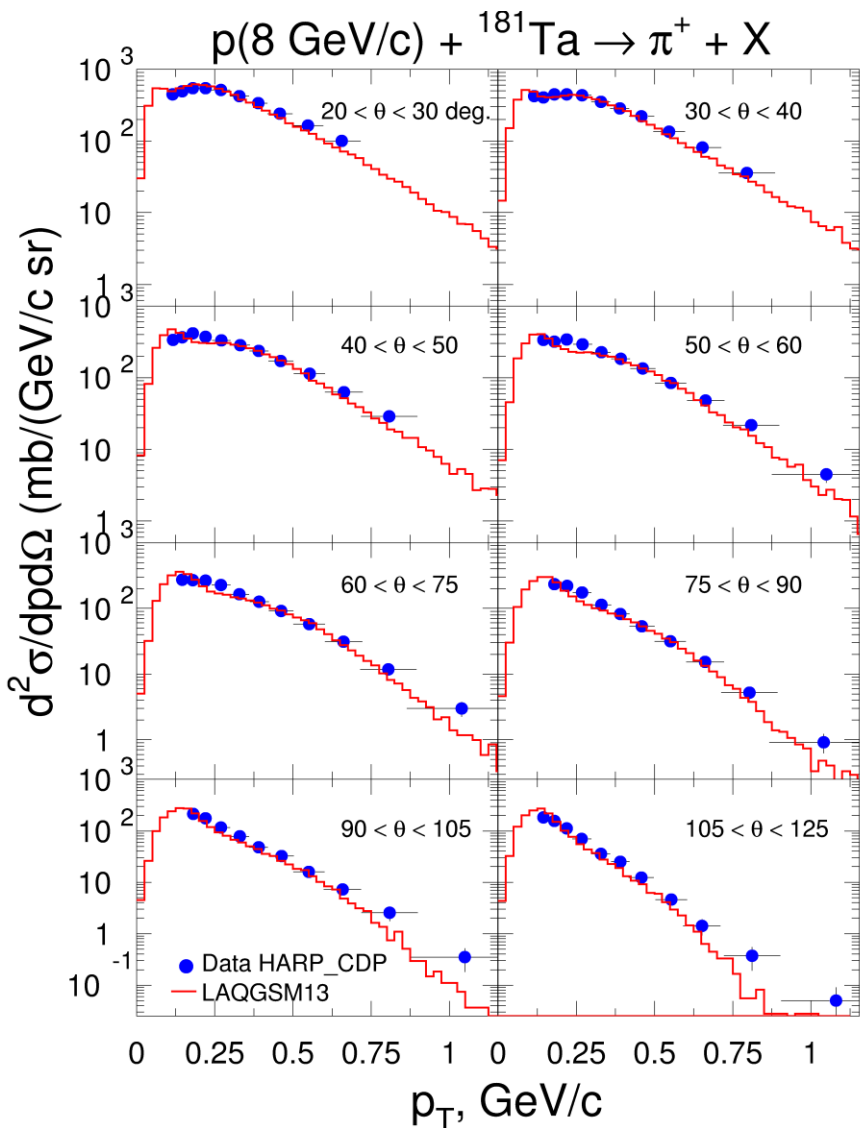
Recent improvements:

- New and better approximations for elementary total, elastic, and inelastic cross sections for NN and π N interactions
- Several channels have been implemented for an explicit description:
 $N+N \rightarrow N+N+m\pi$, $\pi+N \rightarrow N+m\pi$, $B+B \rightarrow B+Y+K$, $\pi+B \rightarrow Y+K$, $K\text{bar}+B \rightarrow Y+\pi$,
and $K+K\text{bar}$, $N+N\text{bar}$ pair production
- Arbitrary light nuclear projectile (e.g., d) and nuclear target (e.g., He)
- Phenomenological parameterization of x-section of pion absorption on NN pair in nuclear medium was constructed based on $\pi+d$ cross section $\sigma(A,T) =$
- $P(A) \times \sigma(\pi+d)$ with $P(A)=\alpha A^\beta$. Absorption probability is proportional to nucleon density squared $\rho^2(r)$
- Improved description of pion absorption in nuclei in $\Delta+N \rightarrow NN$
- New channel for pion production near threshold in $N+N \rightarrow \pi+d$

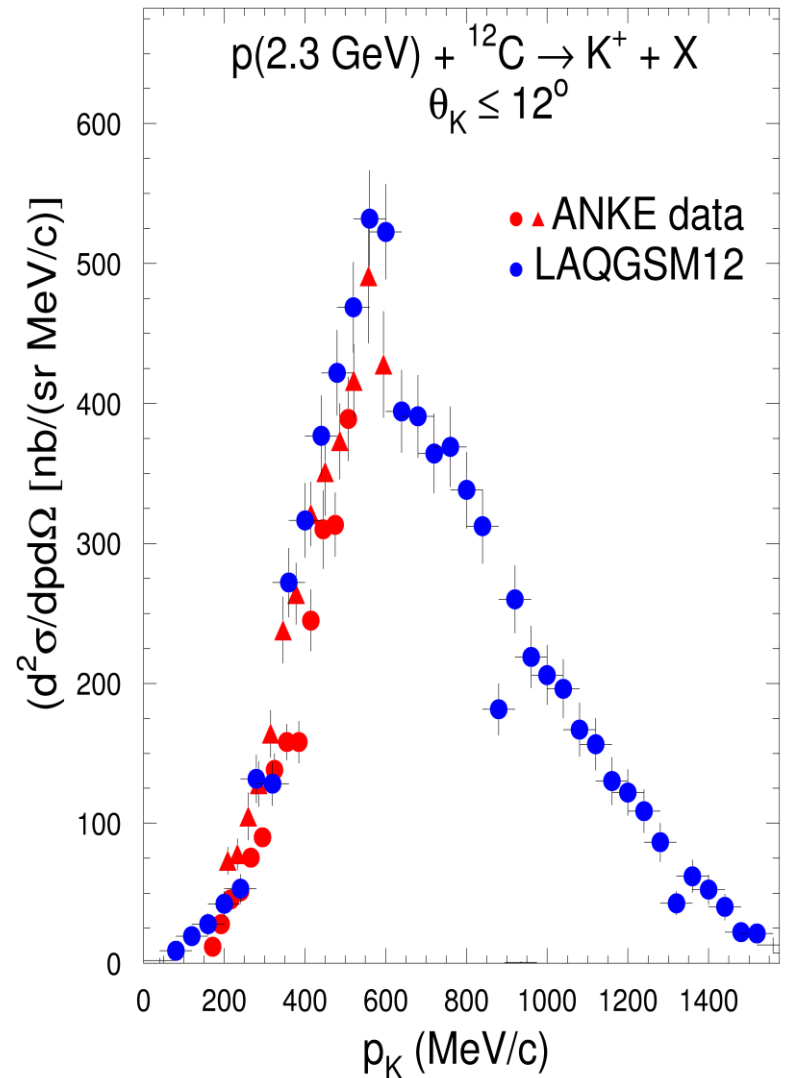
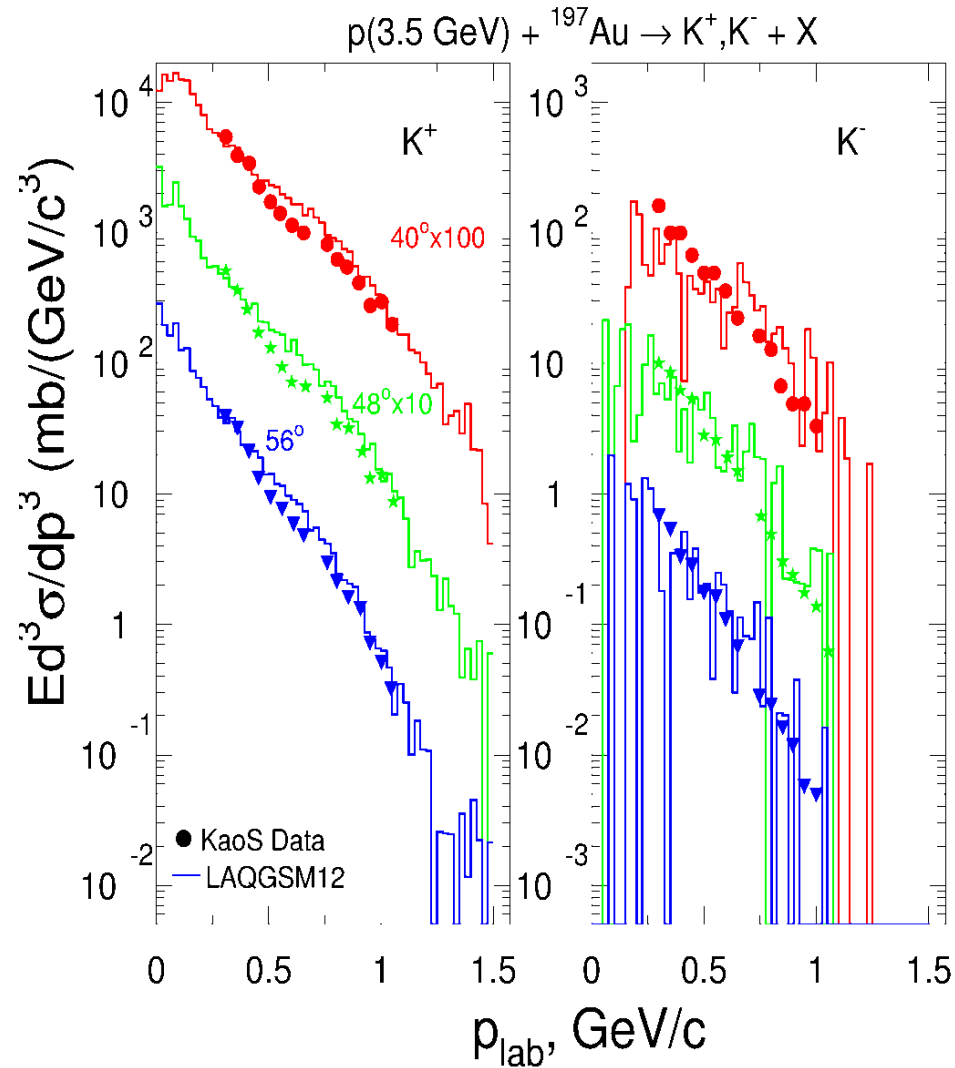
LAQGSM Performance at 585 and 730 MeV



LAQGSM vs HARP-CDP Data at 8 GeV/c

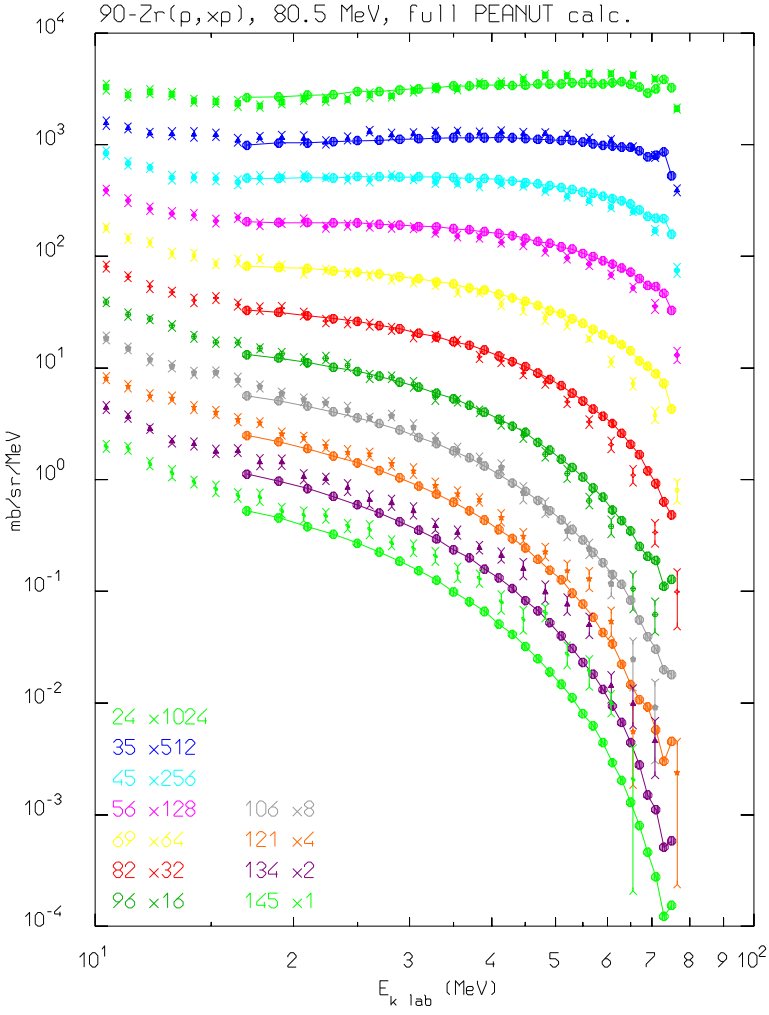


Kaon Production: LAQGSM vs Data



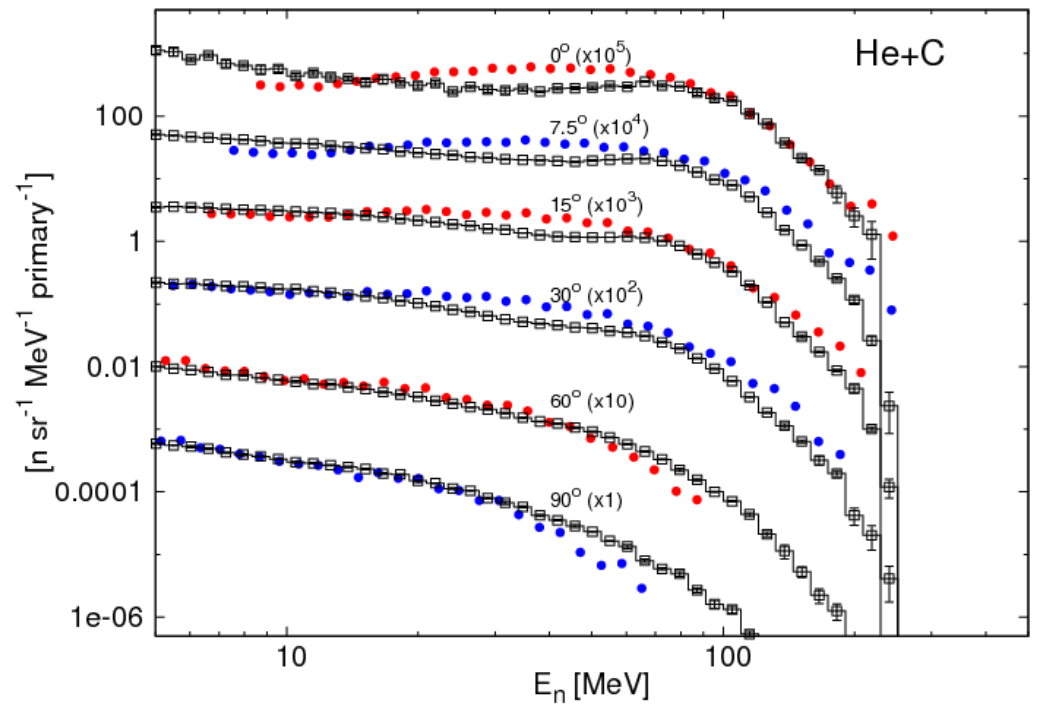
FLUKA Nucleon Production vs Data at 80 & 400 MeV

80 MeV p + ⁹⁰Zr → p + X

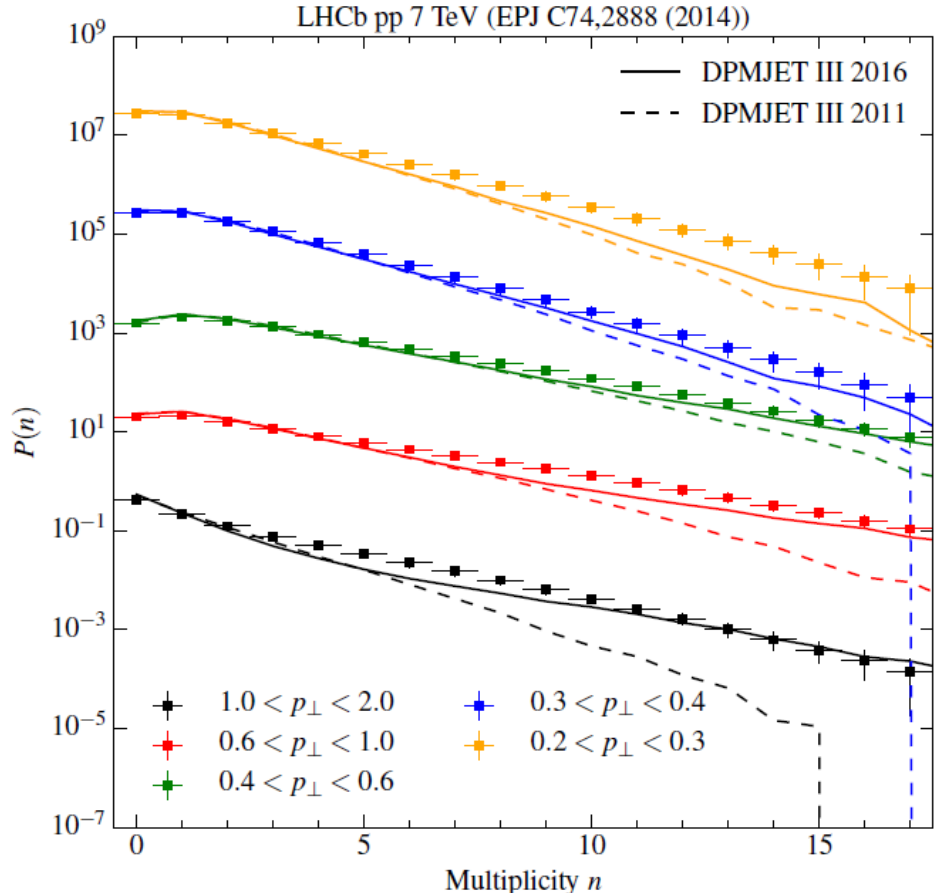


Thick target

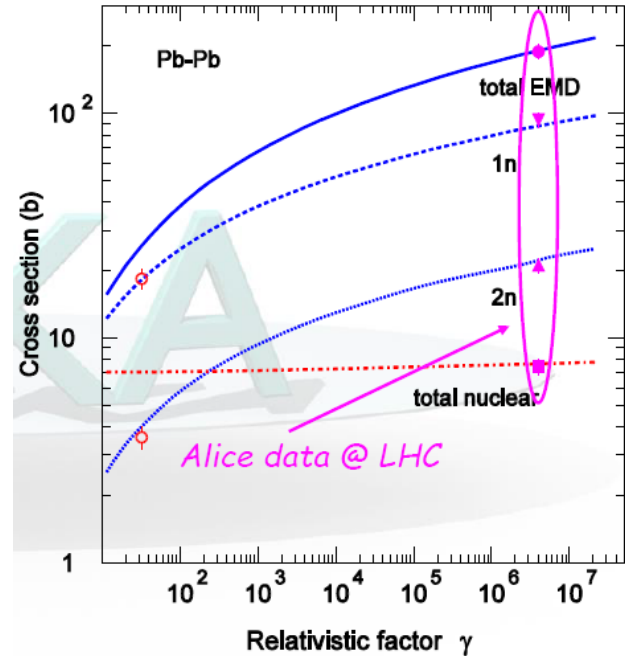
Neutrons from 400 MeV α on carbon



Newest DPMJET III and FLUKA's EMD vs LHC Data



Charged particle multiplicity in pp-collisions at $\sqrt{s} = 7$ TeV integrated over $\eta = 2 - 4.5$ as measured by LHCb (symbols) and simulated with DPMJET-III



Electromagnetic dissociation (EMD) and nuclear x-sections in Pb-Pb collisions: FLUKA vs ALICE data. EMD = very peripheral nuclear interactions thru time-dependent EM field caused by moving nuclei. 1n – one-phonon GDR (high-frequency collective excitation of atomic nuclei, 2n – DGDR (double-phonon giant dipole resonance)

Courtesy A. Ferrari & A. Fedynitch



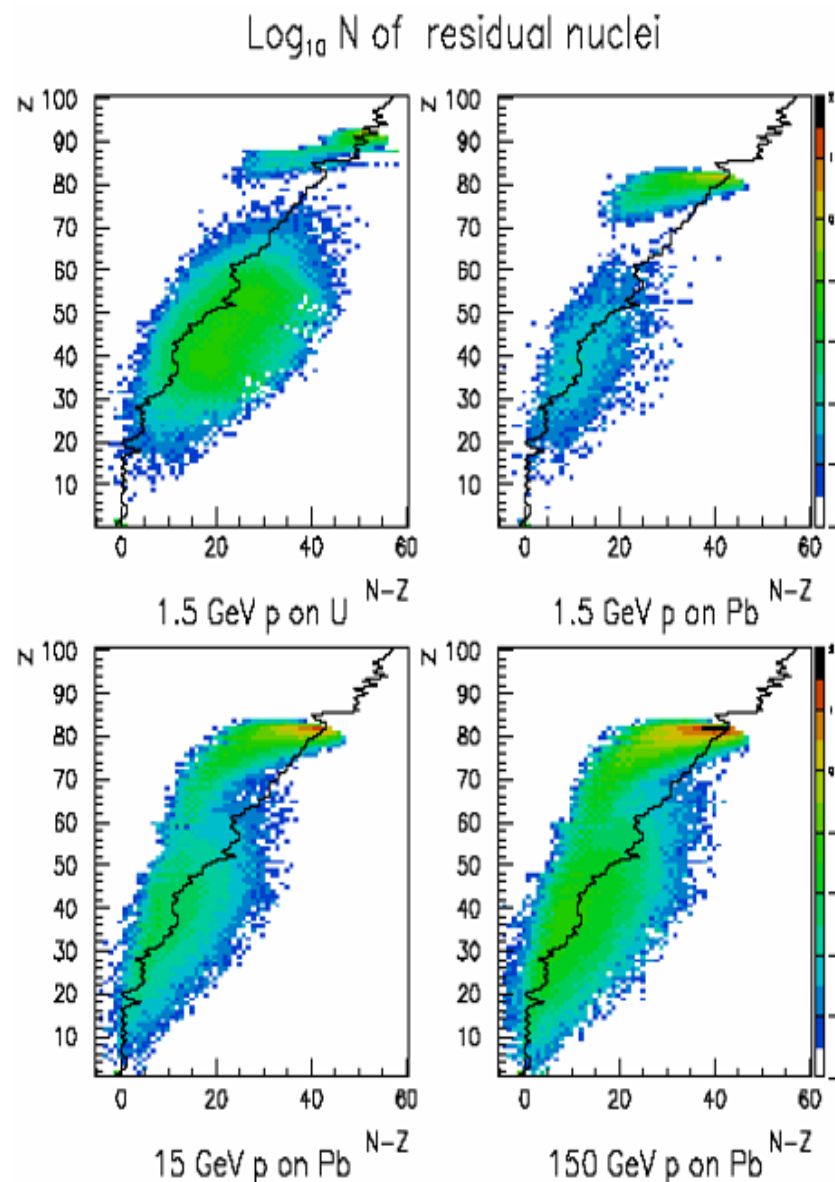
Nuclide Production

The production of residuals is the result of the last step of the nuclear reaction, thus it is influenced by all the previous stages. However, the production of specific isotopes may be influenced by fine nuclear structure effects which have little or no impact on the emitted particle spectra.

After many collisions and possibly particle emissions, the residual nucleus is left in a **highly excited equilibrium state**. De-excitation can be described by **statistical models** which resemble the **evaporation** of “droplets”, actually **low energy particles (p, n, d, t, ^3He , alphas...)** from a “boiling soup” characterized by a “nuclear temperature”. The process is terminated when all available energy is spent \rightarrow the leftover nucleus, possibly radioactive, is now “cold”, with **typical recoil energies of \sim MeV**.

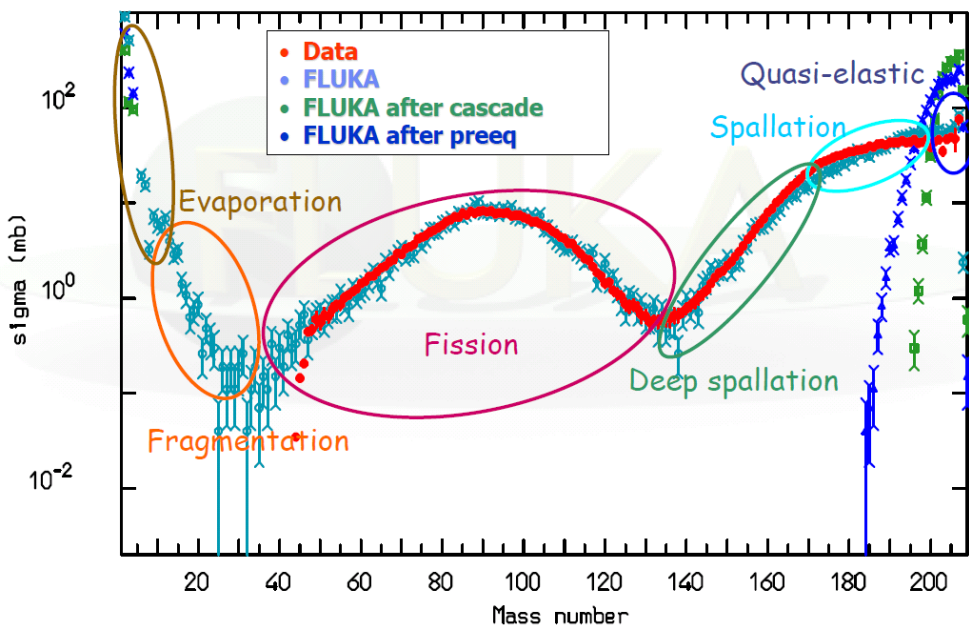
For heavy nuclei, the excitation energy can be large enough to allow breaking into two major chunks (**fission**). Since only neutrons have no barrier to overcome, **neutron emission is strongly favored**.

Courtesy F. Cerutti

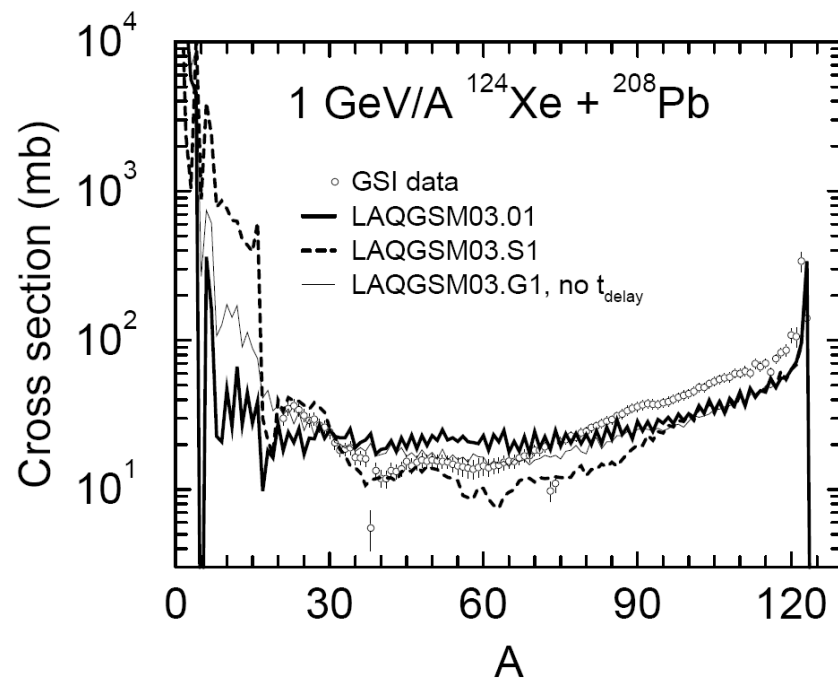


Nuclides from FLUKA & MARS15 Event Generators

FLUKA: 1 GeV/A $^{208}\text{Pb} + \text{p}$

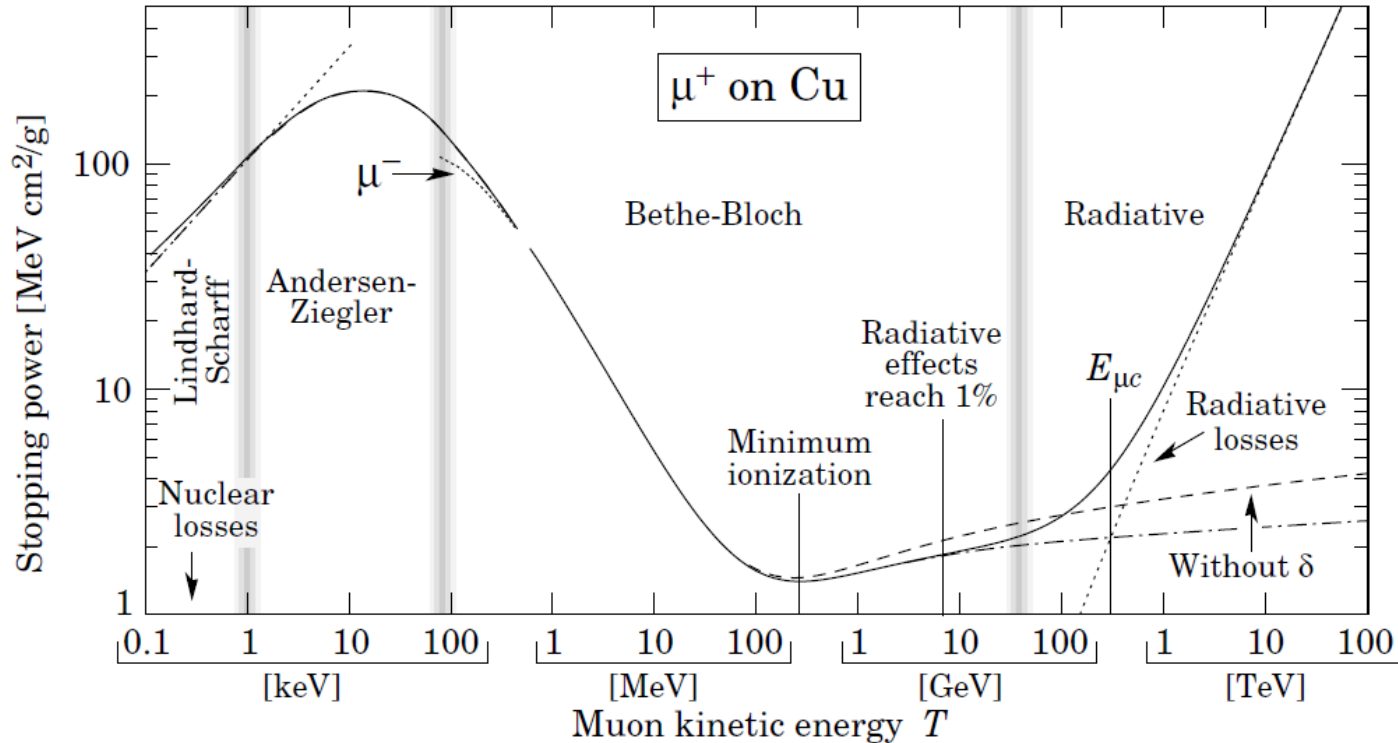


MARS-LAQGSM



Ionization and Radiative Energy Loss dE/dx

Continuous-slowing-down-approximation (CSDA)



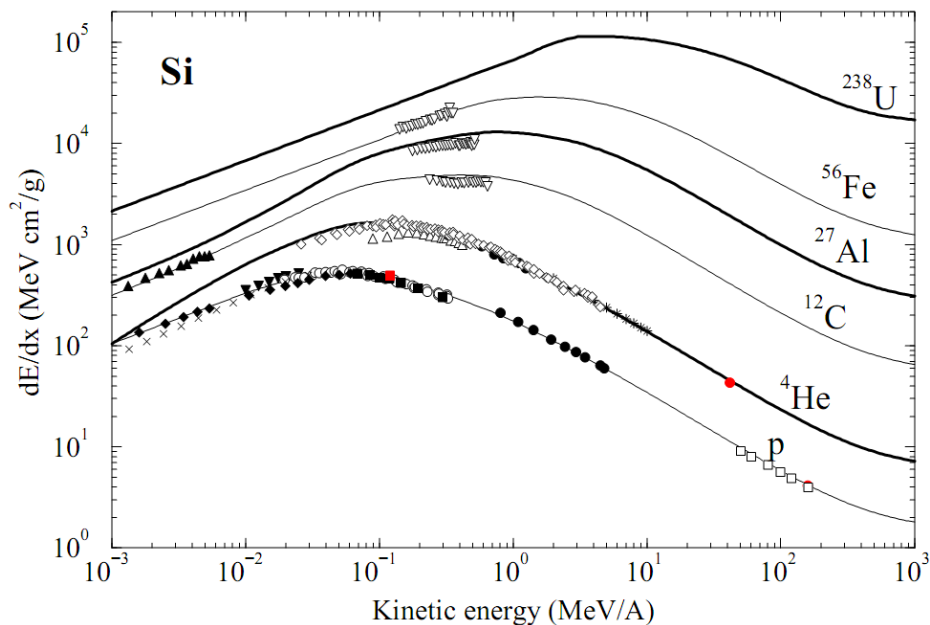
Mean stopping power for charged particles: $(-dE/dx) = a(E) + b(E)E$, where $a(E)$ is the electronic stopping power, and $b(E)$ is due to radiative processes – bremsstrahlung, pair production and photonuclear interactions; both $a(E)$ and $b(E)$ are slowly varying functions of E at high energies

Mean Ionization Stopping Power dE/dx

$$-\frac{1}{\rho} \frac{dE}{dx} = 4\pi N_A r_e^2 m_e c^2 z^2 \frac{Z}{A} \frac{1}{\beta^2} L(\beta)$$

$$L(\beta) = L_0(\beta) + \sum_i \Delta L_i$$

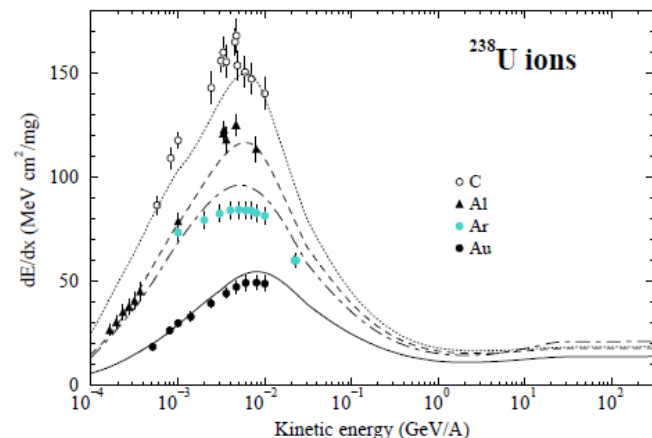
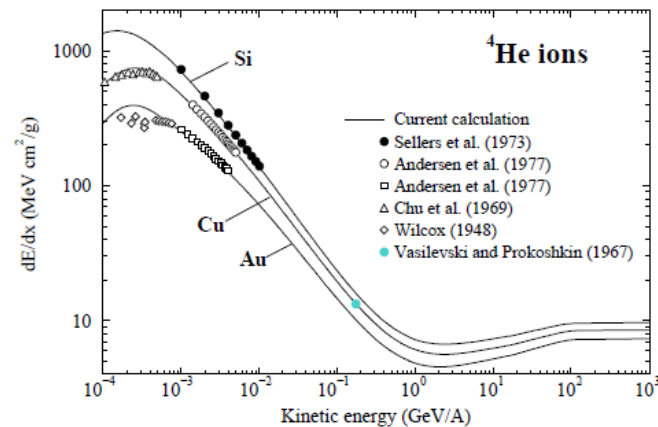
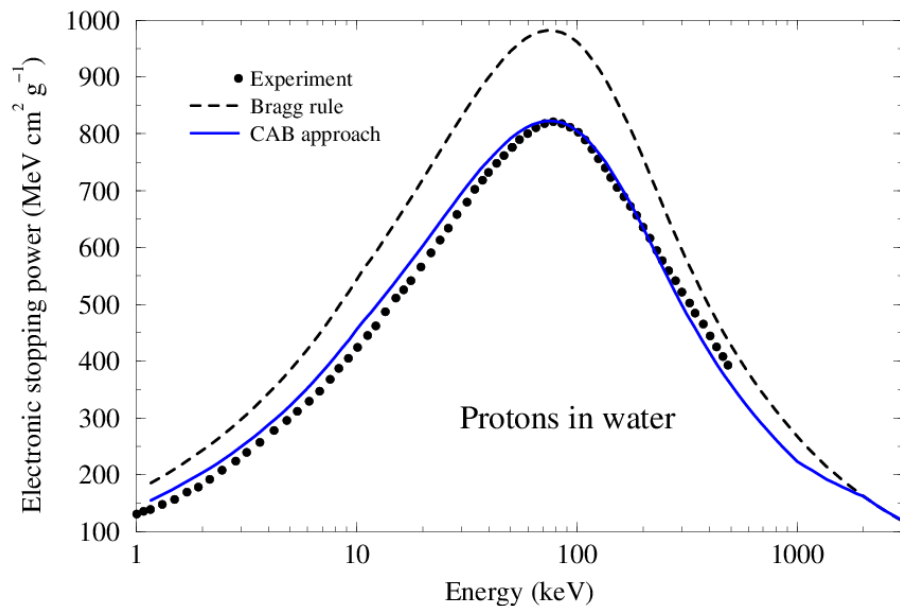
$$L_0(\beta) = \ln\left(\frac{2m_e c^2 \beta^2 \gamma^2}{I}\right) - \beta^2 - \frac{\delta}{2}$$



- ΔL_i : (i) **Lindhard-Sørensen** correction (exact solution to the Dirac equation; terms higher than z^2)
 (ii) **Barkas** correction (target polarization effects due to low-energy distant collisions)
 (iii) **shell** correction

Projectile **effective charge** comes separately as a multiplicative factor that takes into account electron capture at low projectile energies (e.g., $z_{\text{eff}} \sim 20$ for 1-MeV/A ^{238}U in Al, instead of bare charge of 92)

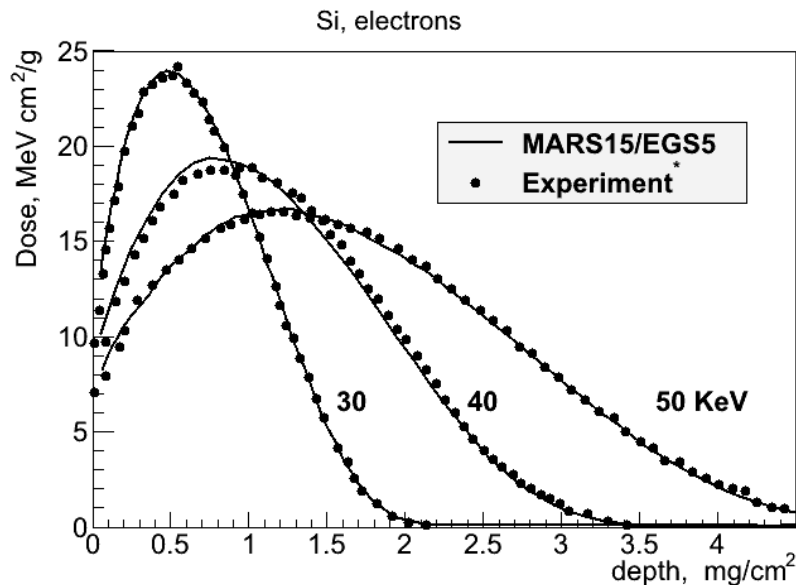
dE/dx: Mixtures and Heavy Ions



Stopping power of ions in compounds usually is described according to Bragg's rule. At low energies and for low-Z materials the difference between measured and predicted dE/dx can be as large as 20%. The "cores-and-bonds" (CAB) method in MARS15 takes into account chemical bonds fitted to experiment for various compounds

Energy Loss and Energy Deposition Modeling

1. The CSDA dE/dx is widely used in quick estimations of energy loss by particle beams and in simplified simulations of energy loss and energy deposition along the charged particle tracks in hadronic and electromagnetic cascades.
2. In a more sophisticated approach used these days in several codes, precise modeling of knock-on electron production with energy-angle correlations taken into account is done for electronic losses.



3. Radiative processes – bremsstrahlung, pair production and inelastic nuclear interactions (via virtual photon) – for muons and high-energy hadrons - are modelled exclusively using pointwise x-sections.

Items (2) and (3) allow precise calculation of 3D energy deposition maps induced by high energy cascades.

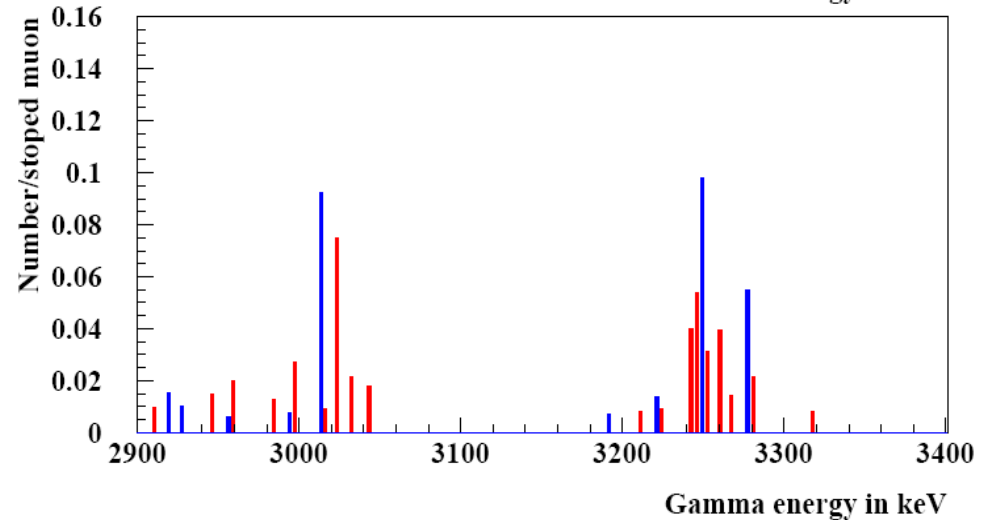
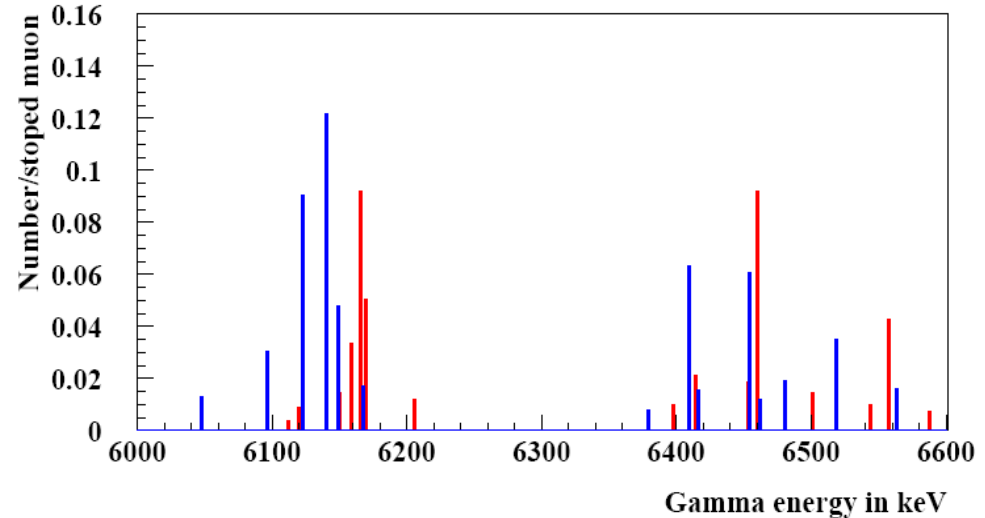
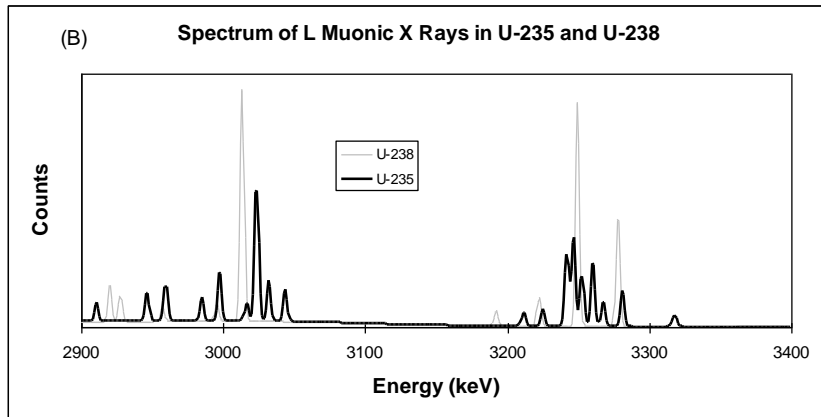
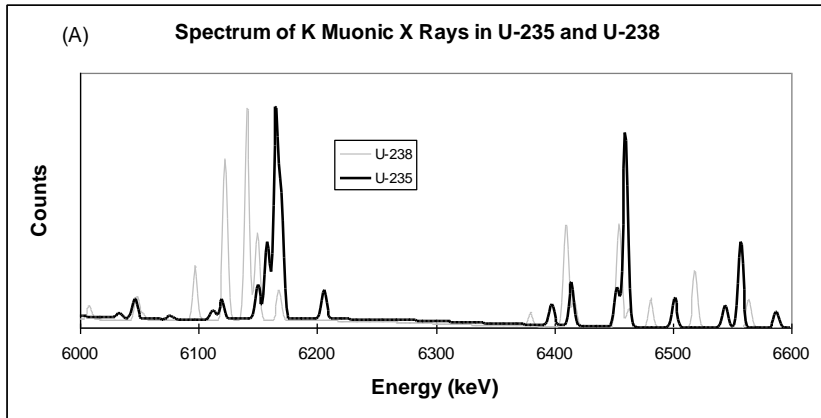
Muons, Neutrinos and Particle Stopping

- Analog and inclusive algorithms are used (in MARS15) for unstable particle decays, prompt muon production (single muons in charmed meson decays, $\mu^+\mu^-$ pairs in vector meson muon decays, and the dimuon continuum), Bethe-Heitler $\mu^+\mu^-$ pairs and direct $e^+e^- \rightarrow \mu^+\mu^-$ annihilation.
- Neutrinos from meson and muon decays are forced to interact with matter in the following processes:
$$\nu_\mu N \rightarrow \mu^+ X, \nu_\mu N \rightarrow \nu_\mu X, \nu_\mu p \rightarrow \mu^+ n, \nu_\mu p \rightarrow \nu_\mu p, \nu_\mu n \rightarrow \nu_\mu n,$$
$$\nu_\mu e^- \rightarrow \nu_\mu e^-, \nu_\mu e^- \rightarrow \nu_e \mu^-, \nu_\mu A \rightarrow \nu_\mu A.$$
- Decays of slowing-down pions and muons and their nuclear capture are carefully modeled in a competition. Antiproton annihilation is modeled exclusively

Stopped Muons

- A stopping μ^+ always decays into positron and neutrinos, while a μ^- attaches itself to a nucleus. When a μ^- stops in a compound or mixture, one first decides to which nucleus it attaches (modified Fermi-Teller law). Following attachment, the muon may still decay as decided by comparing capture and decay lifetimes of which the latter is favored for light nuclei ($Z < 12$).
- A captured μ^- then cascades down to the ground state of the muonic atom emitting photons along with some Auger electrons, all of which are simulated using a corresponding database for the atomic energy levels.
- In hydrogen, muon capture always produces a 5.1-MeV neutron via inverse beta-decay. In complex nuclei, the giant dipole resonance plays a role and results in an “evaporation”-type neutron spectrum with one or more resonances superimposed.

Stopped Muons in Uranium: exp vs MARS15



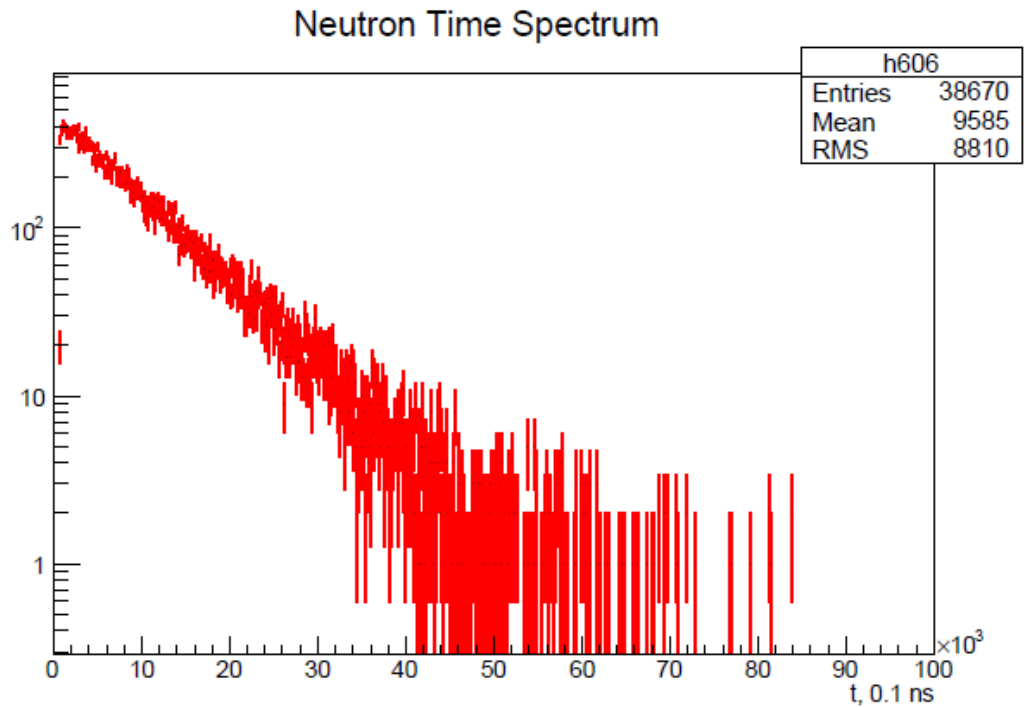
X-rays at muon stop. Red - U^{235} . Blue - U^{238} .

Simulation from experimental data
on μ^- cascade in U^{238} and U^{235}

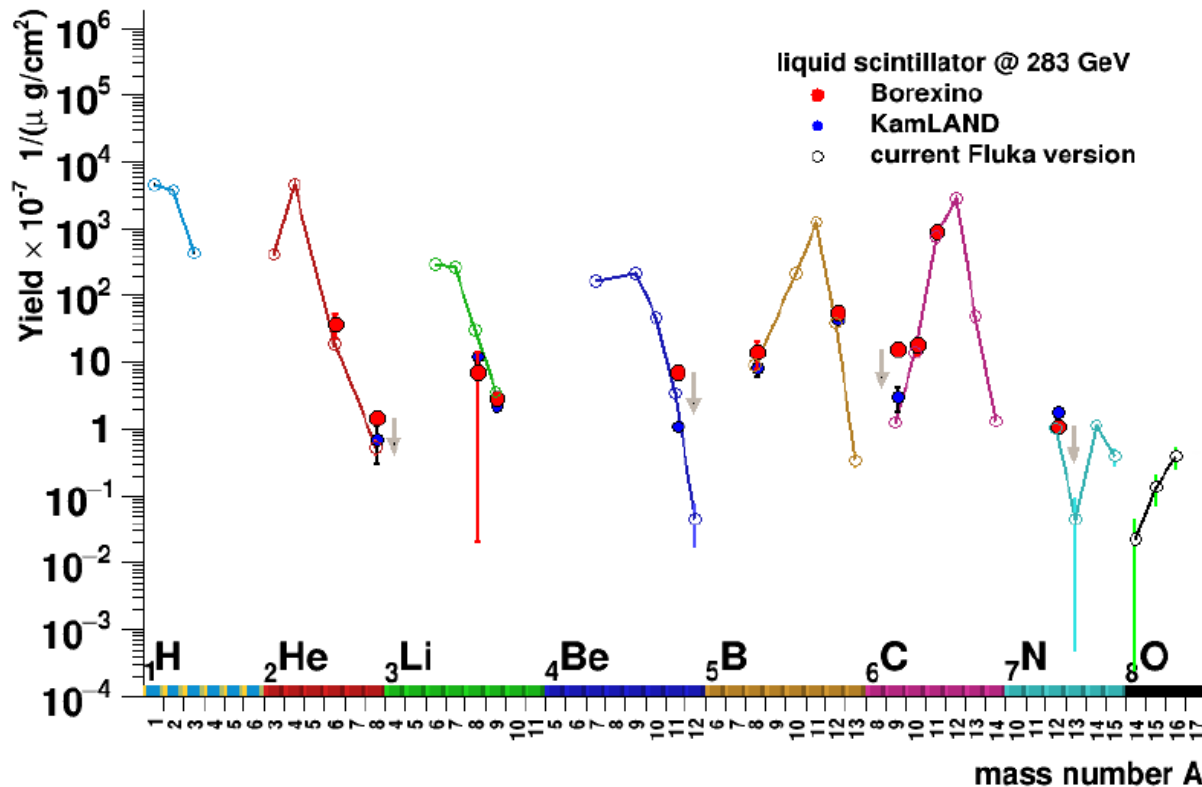
Checking at ports of entry...

Neutron Time Spectrum from Stopped 5-keV μ^- in Al

Neutron and neutrino spectra are MARS15-calculated on the basis of a comprehensive database for muon lifetime at capture and nuclear capture fraction



Muon-Induced Cosmogenic Isotope Production

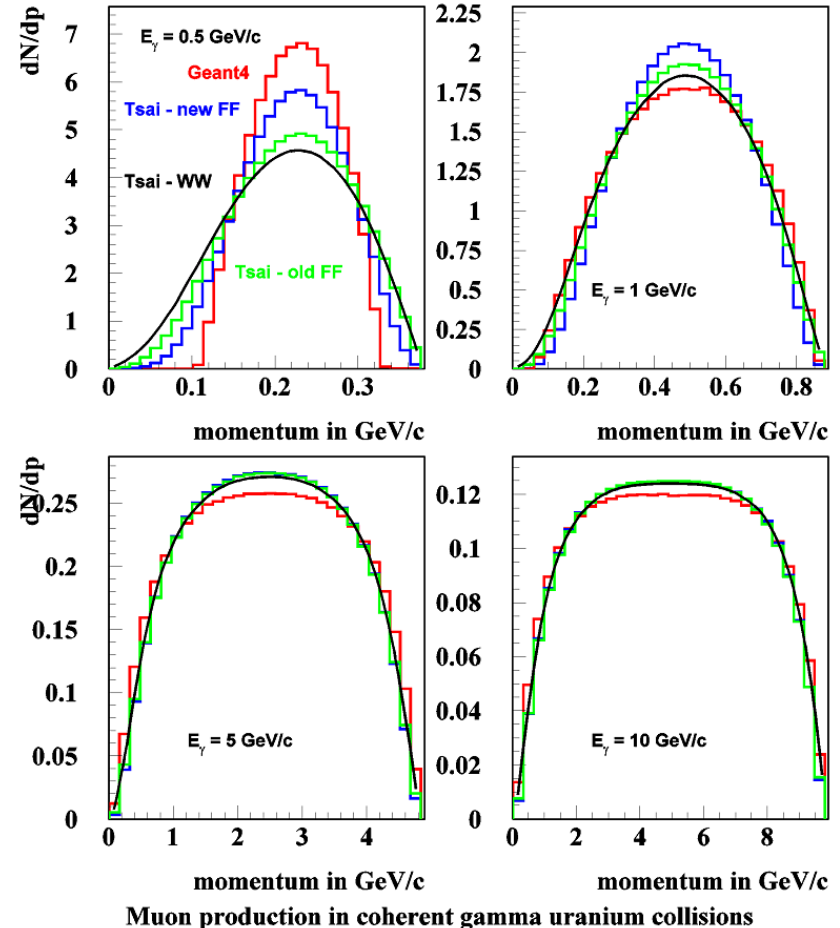
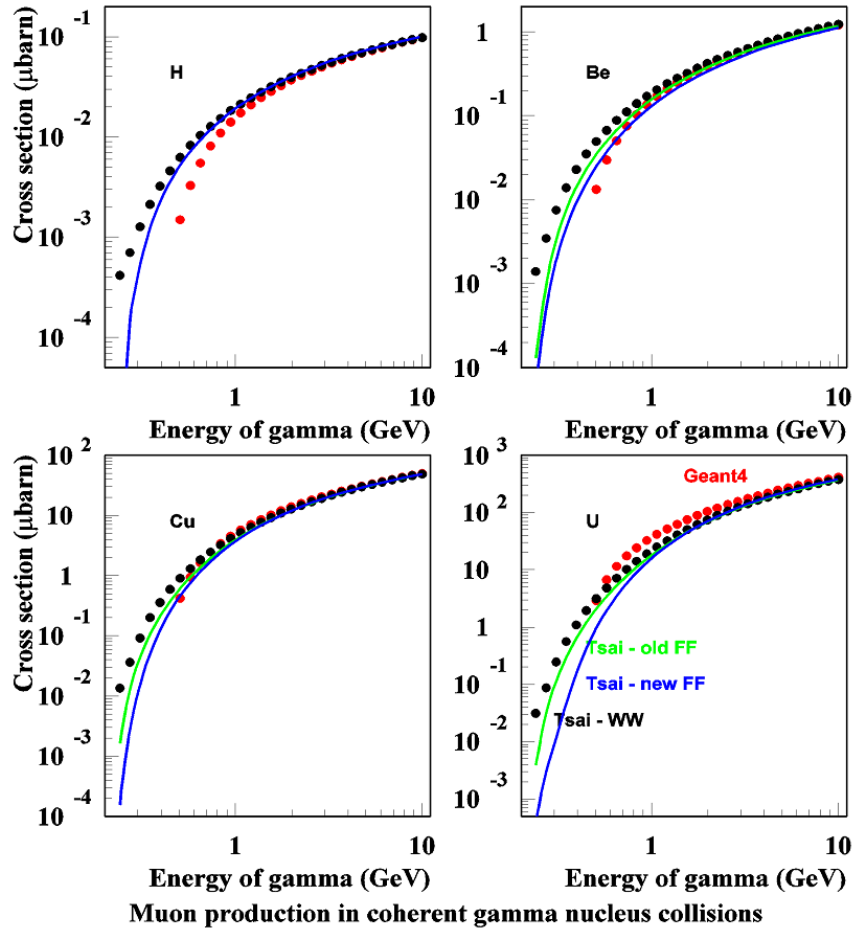


Isotope yields in liquid scintillator underground detectors assuming realistic muon spectra with an average energy of 283 GeV as measured in the Borexino and KamLAND experiments and calculated with FLUKA

Courtesy A. Ferrari & A. Fedynitch

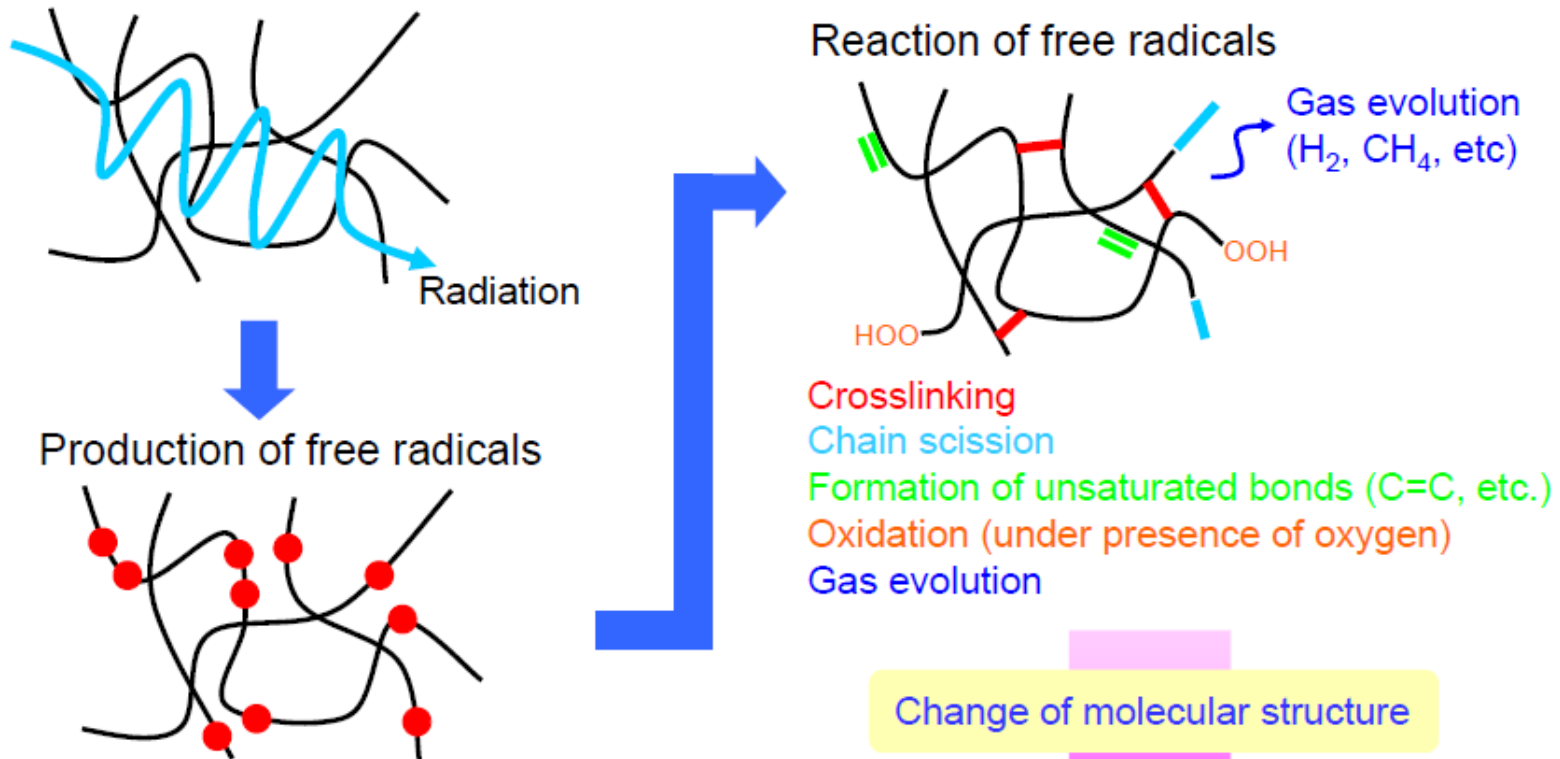
Muon Pair Production in Coherent Low-E γA

Generalized MARS15 model for arbitrary target mass and form-factor with extension at 0.2 to a few GeV photons where Bethe-Heitler model fails



MARS15 (blue lines) labeled “Tsai – new FF”

Interaction of Particles with Organic Materials



For given insulator and irradiation conditions radiation damage is proportional to energy deposition (dose)

Courtesy A. Idesaki

- Irradiation temperature
- Irradiation atmosphere (presence of oxygen)
- Additives

Beam-Induced Effects in Organic Materials

Contrary to the MeV type accelerators with their insulators made mostly of ceramics or glasses, the majority of insulators in high-energy accelerator equipment are made of organic materials: epoxy, G11, polymers etc. Apart from electronics and optical devices, the organic materials are the ones most sensitive to radiation. Radiation test findings:

- Degradation is enhanced at high temperatures.
- Radiation oxidation in presence of oxygen accelerates degradation.
- Radiation oxidation is promoted in the case of low dose rate.
- Additives can improve radiation resistance. For example, 1% by weight of antioxidant in polyethylene can prolong its lifetime 5 to 10 times.

Beam-Induced Effects in Inorganic Materials

- The dominant mechanism of structural damage of inorganic materials is displacement of atoms from their equilibrium position in a crystalline lattice due to irradiation with formation of interstitial atoms and vacancies in the lattice. Resulting deterioration of material critical properties is characterized – in the most universal way - as a function of **displacements per target atom (DPA)**. DPA is a strong function of projectile type, energy and charge as well as material properties including its temperature.
- At accelerators, radiation damage to structural materials is amplified by **increased hydrogen and helium gas production** for high-energy beams. In the Spallation Neutron Source (SNS) type beam windows, the ratio of He/atom to DPA is about 500 of that in fission reactors. These gases can lead to grain boundary embrittlement and accelerated swelling.

Atomic Displacement Cross-Section and NIEL

- Atomic displacement cross section

$$\sigma_d = \sum_r \int_{E_d}^{T_r^{\max}} \frac{d\sigma(E, Z_t, A_t, Z_r, A_r)}{dT_r} N_d(T_r, Z_t, A_t, Z_r, A_r) dT_r$$

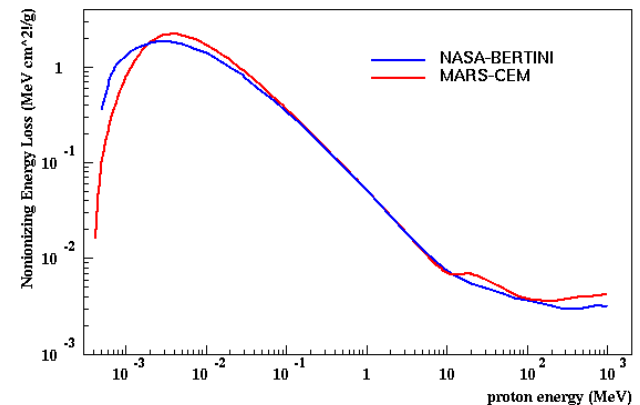
- N_d – number of stable defects produced, E_d – displacement threshold, $d\sigma/dT_r$ - recoil fragment energy (T_r) distribution

- Non-ionizing energy loss (NIEL)

$$\frac{dE}{dx_{ni}} = N \sum_r \int_{E_d}^{T_r^{\max}} \frac{d\sigma(E, Z_t, A_t, Z_r, A_r)}{dT_r} T_d(T_r, Z_t, A_t, Z_r, A_r) dT_r$$

N – number of atoms per unit volume

T_d - damage energy = total energy lost in non-ionizing process (atomic motion)



NRT “Standard” Model to Calculate a Number of Frenkel Pairs and Damage Energy

M.J. Norgett, M.T. Robinson, I.M. Torrens Nucl. Eng. Des 33, 50 (1975)

$$N_d = \frac{0.8}{2E_d} T_d$$
$$T_d = \frac{T_r}{1 + k(Z_t, A_t, Z_r, A_r)g(T_r, Z_t, A_t, Z_r, A_r)}$$

T_r, Z_r, A_r - recoil fragment energy=primary knock-on (PKA) energy, charge and atomic mass

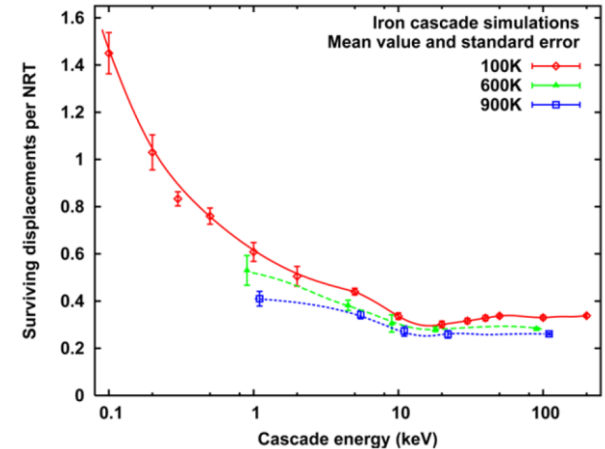
Z_t, A_t - charge and atomic mass of irradiated material

Nuclear physics (T_r, T_d) + solid state physics (N_d)

NRT-DPA is successfully applied to correlate data from many studies involving direct comparison from different irradiation environments

Efficiency Function (1): Stoller MD Parametrization

Corrections to NRT to account for atom recombination in elastic cascading. Database based on MD simulations. Its parametrization, efficiency function $\xi(T) = N_D / N_{NRT}$, is used for several years in MARS15 (=1 if >1, since 2016).



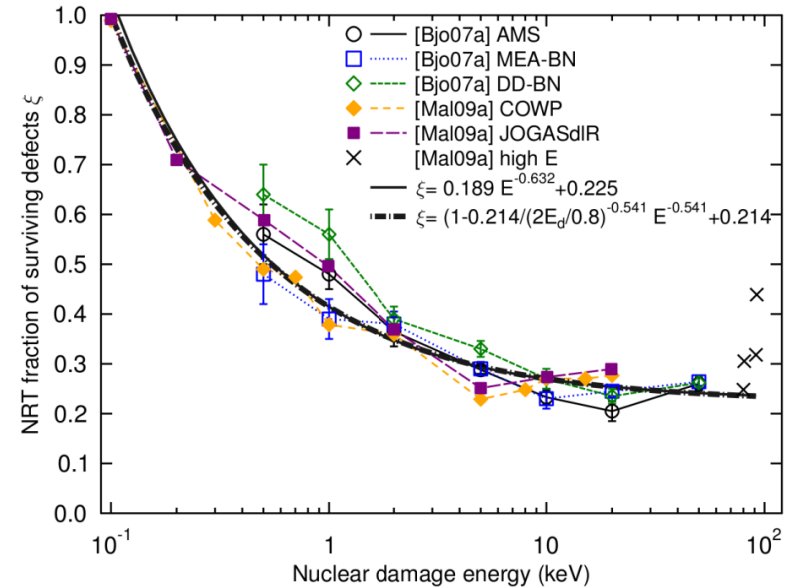
Modest temperature dependence: The calculations of Stoller (J. Nucl.Mater. 276 (2000) 22) for iron at 100-900K show some temperature dependence of the number of stable defects. At the same time, the comparison of Stoller's defect generation efficiency with the displacement cross-sections derived by Jung (J. Nucl. Mater. 117 (1983) 70) from low temperature experiments shows very good agreement.

Efficiency Function (2): Nordlund ARC-DPA

Nordlund's the ARC-DPA concept (athermal recombination-corrected DPA, in MARS15 since 2016):

“The recombination process does not require any thermally activated defect migration (atom motion is caused primarily by the high kinetic energy introduced by the recoil atom), this recombination is called “athermal” (i.e. it would also happen if the ambient temperature of the sample would be 0 K).”

The arc-dpa concept allows empirical validation against frozen defects at cryogenic temperature, whereas NRT is an unobservable quantity.



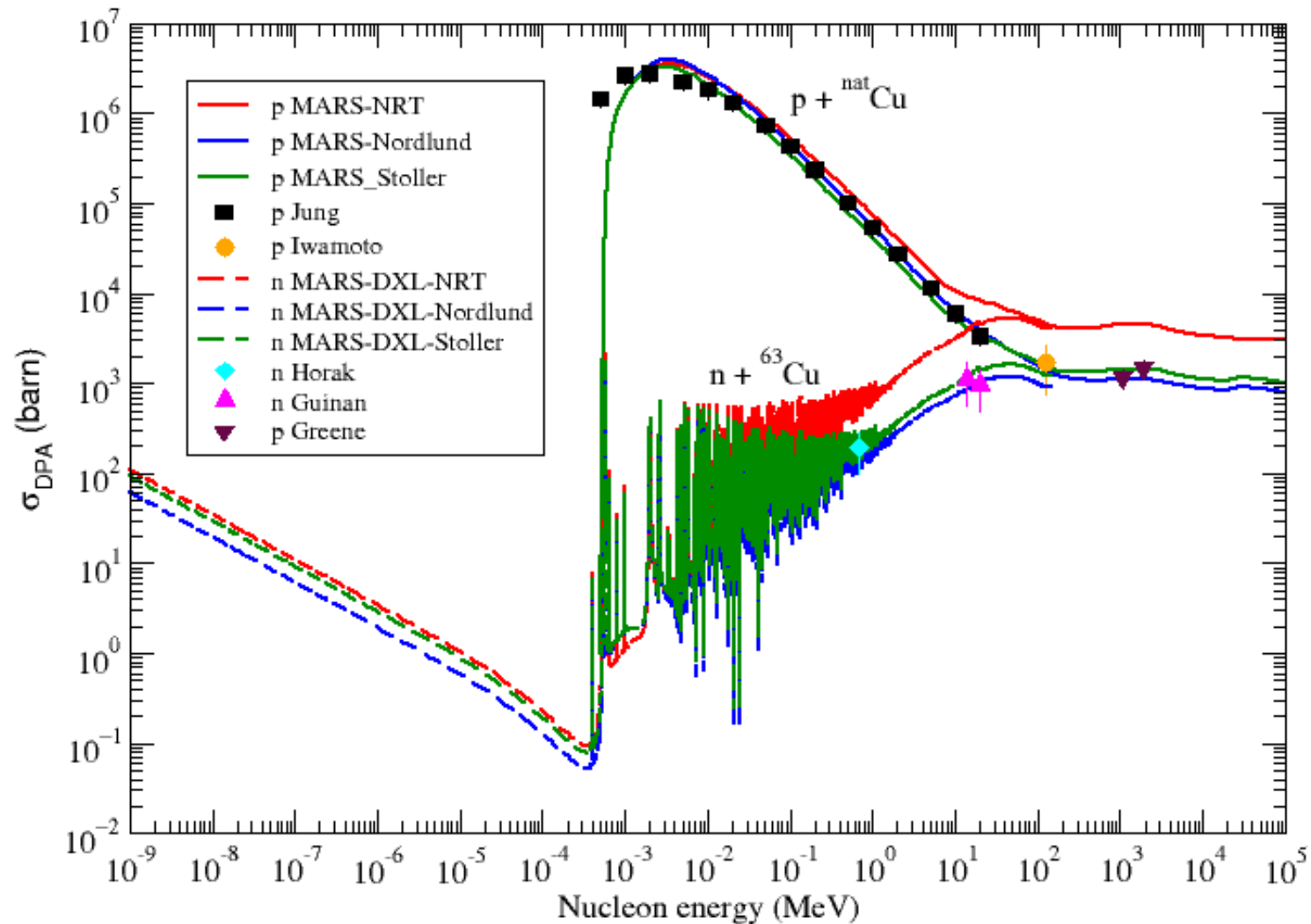
Modified NRT

$$N_d = \begin{cases} 0 & T_d < E_d \\ 1 & E_d < T_d < 2.5E_d \\ \frac{T_d}{2.5E_d} \xi(T_d) & 2.5E_d < T_d \end{cases}$$

with efficiency function

$$\xi(T) = 0.214 + 0.786 \times (2.5E_d / T)^{0.541}$$

Proton & Neutron DPA on Copper: MARS15 vs Data



Accumulated Beam-Induced Effects in Silicon Detectors and Electronics

- **Surface damage:** ionization in SiO₂ layer and at Si-SiO₂ interface
- **Bulk damage:** conventional DPA mechanism, implemented in simulation codes as a 1-MeV (Si) equivalent neutron fluence

$$\Phi_{\text{eq}}^{1\text{MeV}} = \int dE \frac{D(E)}{95\text{MeV mb}} \Phi(E)$$

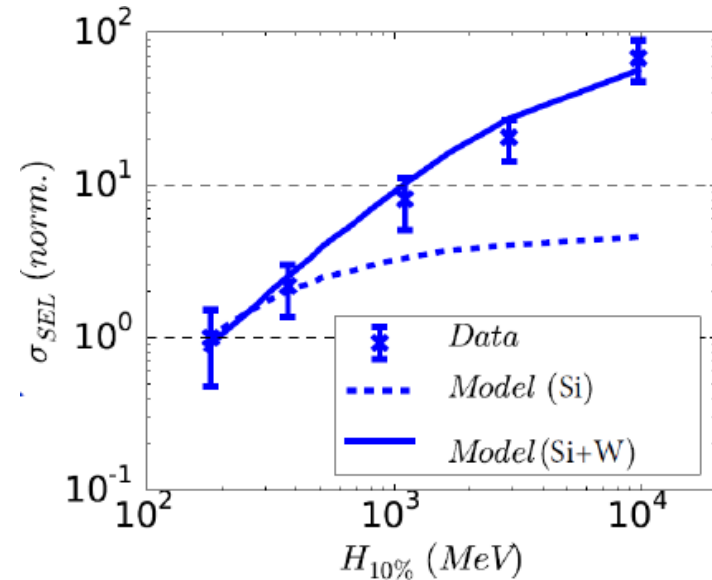
where $D(E)$ is a displacement damage function of any particle for a given energy E , normalized to the one for 1-MeV neutrons (= 95 MeV mb)

Beam-Induced Soft Errors in Silicon Electronics

Single-Event Upset (SEU): a change of state caused by one single ionizing particle (ions, electrons, photons...) striking a sensitive node in a micro-electronic device, such as in a microprocessor, semiconductor memory, or power transistors.

The state change is a result of the free charge created by ionization in or close to an important node of a logic element (e.g. memory "bit").

The error in device output or operation caused as a result of the strike is called an SEU or a soft error.

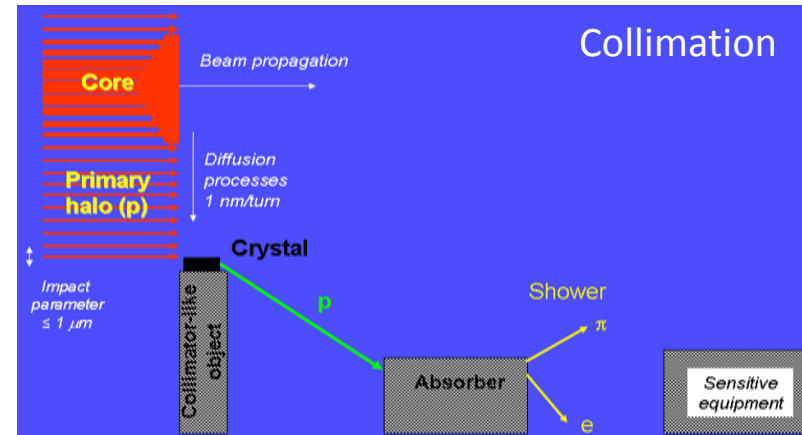
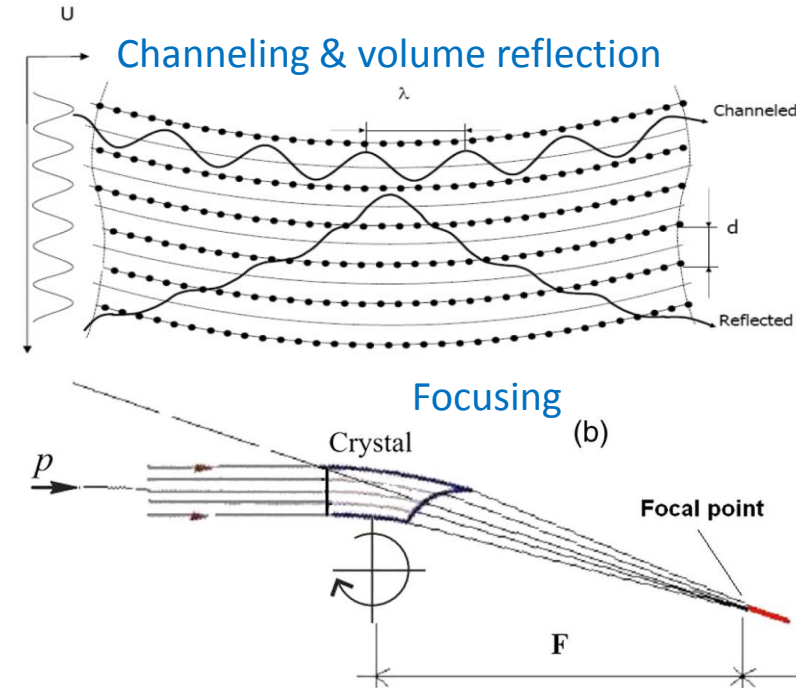


Courtesy A. Ferrari & R. Garcia Alia

CHARM data vs FLUKA model with and w/o heavy materials as a function of spectral hardness (energy above which 10% of the spectrum remains)

Coherent Beam Interactions with Crystals

- Extremely high interplanar electric fields (a few GV/cm) from screened nuclei allow bending of high-energy beams with a few mm thick crystals. Interplanar spacing $\sim 2\text{\AA}$
- Applications: beam extraction, collimation and focusing
- Demonstrated at IHEP U-70, Tevatron, SPS and LHC. Considered for collimation at HL-LHC
- Drastically reduced nuclear interaction rates & energy loss; crystals are heat and radiation resistant
- But setting crystals up at high energies is more challenging compared to a conventional amorphous scatterer



Radiation Damage Issues and Needs

Despite a substantial progress in the field of radiation damage over last several years, there are still several misses and open questions:

- Needs for radiation damage measurements at cryogenic temperatures.
- Measurements with charged particle beams and their relation to neutron data.
- Annealed versus non-annealed defects.
- Low-energy neutron DPA in compounds.
- Consistent link of calculated DPA and a 1-MeV (Si) equivalent neutron fluence to observed changes in materials/electronics properties.
- SEU x-sections and soft error data for specific microelectronics

Status of Particle Production Models

- Particle production models are OK at $E_p < 1$ GeV, $E_p > 10$ GeV and – with recent improvements - up to LHC energies.
- At intermediate energies 1 - 10 GeV, there are some theoretical difficulties and uncertainties in experimental data; the latter contradicts each other in some cases.
- In the above-LHC energy domain, more work is certainly needed to increase the confidence in results and various design proposals for the FCC project in avalanche of recent publications.